Chimeric bovine embryo multiplication with *OCT4* knockout host embryos

von Kilian Manuel Simmet

Inaugural-Dissertation zur Erlangung der Doktorwürde

(Dr. rer. biol. vet.)

der Tierärztlichen Fakultät der Ludwig-Maximilians-Universität München

Chimeric bovine embryo multiplication with *OCT4* knockout host embryos

von Kilian Manuel Simmet

aus Valdivia / Chile

München 2017

Aus dem Veterinärwissenschaftlichen Department der Tierärztlichen Fakultät der Ludwig-Maximilians-Universität München

Lehrstuhl für Molekulare Tierzucht und Biotechnologie

Arbeit angefertigt unter der Leitung von Univ.-Prof. Dr. Eckhard Wolf

Mitbetreuung durch: Dr. Nikolai Klymiuk und Prof. Dr. Valeri Zakhartchenko

Gedruckt mit Genehmigung der Tierärztlichen Fakultät

der Ludwig-Maximilians-Universität München

Dekan:	Univ.-Prof. Dr. Joachim Braun
Berichterstatter:	Univ.-Prof. Dr. Eckhard Wolf
Korreferent/en:	Prof. Dr. Sabine André
	Priv.-Doz. Dr. Petra Kölle
	Univ.-Prof. Dr. Dr. h.c. Hans-Joachim Gabius
	Univ.-Prof. Dr. Gerd Sutter
Tag der Promotion:	11.02.2017

Meinen lieben Eltern

TABLE OF CONTENTS

INDEX OF ABBREVEATIONS

BME	Basal medium Eagle’s amino acids solution
bp	Basepairs
CDX2	Caudal type homeobox 2
CLSM	Confocal laser scanning microscope
COC	Cumulus–oocyte complex
CR4	Conserved region 4
CRISPR	Clustered regulatory interspaced palindromic repeats
crRNA	CRISPR RNA
DAPI	4′,6-Diamidino-2-phenylindole
DMEM	Dulbecco's Modified Eagle Medium
DNA	Deoxyribonucleic acid
dNTP	Nucleoside triphosphate
DSB	Double strand break
DTT	1,4-dithiothreitol
EDTA	Ethylenediaminetetraacetic acid
EGA	Embryonic genome activation
eGFP	Enhanced green fluorescent protein
EGTA	Ethylene glycol-bis(β-aminoethyl ether)-N,N,N′,N′-tetraacetic acid tetrasodium salt
EPI	Epiblast
ESC	Embryonic stem cells
ETF1	Eukaryotic translation termination factor 1
FCS	Fetal calf serum

FGF4	Fibroblast growth factor 4
FGFR	Fibroblast growth factor receptor
FSH	Follicle stimulating hormone
GATA3	GATA binding protein 3
GATA6	GATA binding protein 6
GEBV	Genomic estimated breeding value
gRNA	Guide RNA
HB	Hypoblast
HDR	Homology directed repair
hep	Heparin
ICM	Inner cell mass
indel	Insertion or deletion
iPSC	Induced pluripotent stem cells
IVF	*In vitro* fertilization
IVM	*In vitro* maturation
IVP	*In vitro* produced
KO	Knockout
LH	Luteinizing hormone
MAPK	Mitogen-activated protein kinase
MEM	Minimum essential medium
MOET	Multiple ovulation embryo transfer
MSTN	Myostatin
NANOG	Nanog homeobox
NHEJ	Non-homologous end-joining repair
OCS	Estrous cow serum

OCT4	Octamer-binding transcription factor-4
PAM	Protospacer adjacent motif
PBS	Phosphate buffered saline
PCR	Polymerase chain reaction
PE	Primitive endoderm
PGCs	Primordial germ cells
PHA	Phytohemagglutinin-L
PVA	Polyvinyl alcohol
RNA	Ribonucleic acid
SCNT	Somatic cell nuclear transfer
SD	Standard deviation
SDS	Sodium dodecyl sulfate
sgRNA	Small guiding RNA
SNP	Single nucleotide polymorphisms
SOF	Synthetic oviductal fluid
Sox17	Sex determining region Y-box 17
Sox7	Sex determining region Y-box 7
TALEN	Transcription activator-like effector nucleases
TE	Trophectoderm
TL-HEPES-PVA	HEPES-buffered Tyrode's medium with PVA
tracrRNA	Trans-activating RNA
Tris	Tris-(hydroxymethyl)-aminomethane
WoW	Well of the well
ZFN	Zinc-finger nucleases
ZP	*Zona pellucida*

I. Introduction

The advent of genomic selection using single nucleotide polymorphisms (SNP) revolutionized breeding schemes in cattle (HAYES et al., 2009). Provided that enough data on the phenotypes and genotypes of several generations is included, the genomic estimated breeding value (GEBV) even exceeds the traditional EBV in accuracy (MUIR, 2007), while simultaneously the generation interval and the costs of genetic progress are dramatically reduced (SCHAEFFER, 2006). The genotype of an individual is fixed at the time of fertilization, so the GEBV of an embryo is as valid as the GEBV from animals of any age (SEIDEL, 2009). This development may lead to individual embryos from multiple ovulation embryo transfer (MOET) or *in vitro* production with great commercial value due to a high GEBV. A biopsy of ~10 cells, which is necessary to generate a GEBV, unfortunately compromises the embryo. This leads to decreased pregnancy rates after transfer to recipients, especially after cryopreservation (CENARIU et al., 2012; PONSART et al., 2014). Therefore, the multiplication of commercially valuable embryos is highly desired, mostly to ensure that a pregnancy with the promising genotype is established. Different multiplication strategies have been developed, including embryonic cell nuclear transfer (ZAKHARTCHENKO et al., 1995) and the production of monozygotic twins through blastomere separation (TAGAWA et al., 2008), but both methods have not been used commercially because of technically demanding protocols and low efficiencies, respectively.

Alternatively, embryos may be multiplied by chimeric complementation, where a few pluripotent progenitor cells from a genetically valuable donor embryo are combined with host embryos to form the inner cell mass (ICM) and later give rise to the embryo proper, whereas host embryos preferentially contribute to the trophectoderm (TE) and thus form extraembryonic tissues. To exclude host embryos from the ICM, they are e.g. manipulated by electrofusion at the two-cell stage (HIRIART et al., 2013). Still, host embryos that are definitely not able to contribute to the ICM and therefore guarantee non-chimeric offspring with the desired genotype are not available.

One objective of this thesis was to develop an embryo multiplication method using chimeric complementation with host embryos that do not contribute to the ICM. To achieve that, first an aggregation technique with wild-type host embryos was established, which reliably generated transferable blastocysts from the chimeric constructs. Second, genetically modified host embryos that are unable to maintain a pluripotent state and therefore cannot contribute to the embryo proper, were produced by knockout (KO) of the pluripotency regulating transcription factor *OCT4* (*POU5F1*). At the same time, this is the first knockout study to investigate the function of *OCT4* in bovine preimplantation embryos, so additionally this thesis sets out to describe the phenotype of bovine *OCT4* KO embryos and the effect of an *OCT4* KO during the first and the second lineage differentiation.

Parts of this dissertation have been published and were presented at conferences:

Simmet K, Reichenbach M, Reichenbach H-D, Wolf E. Phytohemagglutinin facilitates the aggregation of blastomere pairs from Day 5 donor embryos with Day 4 host embryos for chimeric bovine embryo multiplication. Theriogenology 2015a; 84: 1603-10.

Simmet K, Reichenbach M, Jung S, Fries R, Grupp T, Gschoederer C, Scherzer J, Reichenbach H, Wolf E (2015b) Phytohemagglutinin (PHA) influences blastocyst rate and contribution of donor cells to the inner cell mass of asynchronous bovine embryo aggregation chimeras. Reproduction in Domestic Animals. 16-

Simmet K, Reichenbach M, Jung S, Fries R, Grupp T, Gschöderer C, Scherzer J, Reichenbach H, Wolf E (2015c) 84 Pairs of blastomeres from bovine day 5 morulae are able to contribute to inner cell mass and trophectoderm in chimeric embryos generated by aggregation with two day 4 morulae. Reproduction, Fertility and Development. 135-

Simmet K, Klymiuk, N., Zakhartchenko, V., Güngör, T., Reichenbach, M., Reichenbach, H.D., & Wolf, E. (2016) OCT4 (POU5F1) has no influence on the ratio of inner cell mass to trophectodermal cells in cloned bovine day 7 blastocysts. In: 18th International Congress on Animal Reproduction, ICAR 2016, Tours, France

II. Review of Literature

1. Chimeric embryos

By definition, a chimera is an organism composed from two or more different zygotic cell lines (ANDERSON et al., 1951). In contrast, mosaicism is the presence of genetically distinct cell lines in one organism, which derived from one single zygote (COTTERMAN, 1956).

There are several forms of naturally occurring chimerism. Blood chimerism occurs when dizygotic twins share common blood vessels during their development *in utero* or fetal-maternal blood interchange develops, so hematopoietic stem cells seed mutually in the twins or in the fetus and mother, resulting in a chimeric hematopoietic system. Dispermic chimerism is the aggregation result of two or more different zygotes, which grow into one single body. Several case studies on this rare condition have been reported in humans, which are usually detected by sexual abnormalities (SAWAI et al., 1994; REPAS-HUMPE et al., 1999; RINKEVICH, 2001). A germ line chimera, or germ line parasitism, develops, when the primordial germ cells (PGCs) of one organism reach the gonads of another and colonize them, so germ cells later stem from a different organism (RINKEVICH, 2001), which was already observed in cattle (OHNO et al., 1962).

The first chimeric embryo produced by manipulation was reported by TARKOWSKI (1961), who joined two 8-cell mouse embryos and transferred developed blastocysts to recipients, resulting in live offspring. Since then, embryonic chimeras served as useful tools to study the early development and cell differentiation in mammalian embryos. For instance, several studies used mouse chimeras to investigate the totipotency of distinct cell populations in morulae (inside and outside cells) at different time points of development, concluding that up to the 32-cell stage, all cells can still differentiate into all three cell lineages and are therefore totipotent (SUWIŃSKA et al., 2008; TARKOWSKI et al., 2010). Also the degree of differentiation in bovine trophectodermal cells was examined, which are surprisingly still able to contribute to the ICM of a chimeric blastocyst and thus are capable of changing their cell fate in a new environment (BERG et al., 2011).

The complementation of a tetraploid blastocyst with pluripotent cells gives irrefutable proof of pluripotency, if the added cells contribute to the three germ cell layers and to the germ line cells. A tetraploid blastocyst is produced by electro-fusion at the two-cell stage, addition of a diploid nucleus to a zygote or inhibition of cytokinesis before the first cleavage (EAKIN & BEHRINGER, 2003). In species, where embryonic stem cells (ESC) and induced pluripotent stem cells (iPSC) exist, chimeric complementation is also used to produce genetically modified animals. The pluripotent cells are modified, e.g. by gene targeting, and then injected into a tetraploid blastocyst where they colonize the ICM, which results in chimeric offspring. If the genetically modified cells also develop into germ line cells, the chimeric animals can produce offspring carrying the desired modification (NAGY et al., 1990; PASCOE et al., 1992; KANG et al., 2009; ZHAO et al., 2009).

The first bovine chimeras were produced by injection of ICM cells to day 7 blastocysts, by aggregation of day 5 morulae and by microsurgical combination of half day 5 embryos (up to four halves) within an empty *zona pellucida* (ZP). Both techniques resulted in live chimeric offspring, amongst others documented by chimeric coat colors, as shown in Figure 1 (SUMMERS et al., 1983; BREM et al., 1984).

Figure 1: Chimeric calf from microsurgical combination of half day 5 embryos. Adapted from BREM et al. (1984).

Subsequently, ICMs from different developmental stages (day 8, 10 or 14) were aggregated with day 5.5 morulae, but only ICMs from day 8 and 10 blastocysts were able to contribute to chimeric embryos and additionally live chimeric calves were exclusively born from chimeric embryos with ICMs from day 8. The authors concluded, that aggregation partners cannot overcome a developmental gap of more than 3 days (PICARD et al., 1990). To test the possibility of producing transgenic animals via chimeric complementation of pluripotent transgenic cells with embryos, bovine ES-like cells were microinjected with DNA or ES-like cells were derived from ICMs of embryos reconstructed from transgenic fibroblasts via somatic cell nuclear transfer (SCNT). Day 3 morulae were injected with these pluripotent transgenic cells and live calves were born from both approaches, showing transgene integration in at least one tissue including the gonadal tissue in one calf. Nevertheless, a low transfection efficiency and poor developmental rates of embryos prevented further use of this approach (CIBELLI et al., 1998). Also, aggregation of ES-like cells with tetraploid 8-cell embryos produced by electrofusion at the two-cell stage could not increase the efficiency in production of live chimeric offspring (IWASAKI et al., 2000).

2. Multiplication of embryos through chimeric complementation

When embryonic chimeras are produced with the intention to promote a certain lineage in the offspring, e.g. a transgenic or a desired genotype, measures are taken to drive a host embryo to differentiation towards the extraembryonic tissues. Simultaneously, these strategies increase the colonization of the ICM by a donor embryo or pluripotent cells, so a greater proportion of the embryo proper emerges from the desired genotype. Multiplication of elite embryos by the production of aggregation chimeras is based on the concept, that few blastomeres of a donor embryo form the ICM, whereas host embryo cells preferentially contribute to the TE during the first lineage differentiation to support development of the donor. Thereby several chimeras, that later contain cells from the elite embryo in the ICM, may be produced from a single donor embryo. This helps to ensure pregnancy with an elite genotype and to multiply offspring of a single mating.

Differentiation of the host embryo to TE may be achieved by asynchronous aggregation or use of host embryos with chromosomal aberrations. In asynchronous aggregation, the developmentally more advanced aggregation partner is prone to contribute to the ICM, excluding the host embryo from the pluripotent lineage. Calves from aggregation of a day 8 ICM and a day 5.5 morula predominantly showed the phenotype of the ICM (PICARD et al., 1990). Also, aggregation of a single eGFP positive blastomere from a day 3 embryo with either synchronous (day 3) or asynchronous (day 2) host embryos resulted in 0% integration of the donor blastomere to the ICM in synchronous aggregation vs. 22% in the asynchronous aggregation (HIRIART et al., 2013). In the mouse, it is state of the art to use tetraploid host embryos, i.e. embryos with chromosomal aberrations. Such embryos, produced by electro-fusion at the two-cell stage, show a uniformly tetraploid karyotype (EAKIN & BEHRINGER, 2003) and viable mice completely derived from ESCs may be obtained after chimeric aggregation (NAGY et al., 1993). This is based on the principle that blastomeres with an abnormal karyotype are preferentially allocated in the TE (IWASAKI et al., 1992; NAGY et al., 1993; VIUFF et al., 2002). Production of tetraploid embryos in the bovine is less successful regarding uniform tetraploidy and complementation with ES-like cells (IWASAKI et al., 1989; CURNOW et al., 2000; IWASAKI et al., 2000) and it has been reported, that

embryos fused at the two-cell stage even contain a higher number of diploid blastomeres than non-fused ones. This particular study also did not detect any significant differences between chimeras with fused or non-fused hosts regarding integration of the donor cell to the ICM or the overall blastocyst (HIRIART et al., 2013). Preimplantation embryos with chromosomal aberrations can be identified using their developmental kinetics. Several parameters, such as timing of first and second cleavage, have been determined to select the developmentally most competent embryos produced *in vitro*. In turn, those thresholds can also be used to obtain host embryos containing a high percentage of blastomeres with an abnormal karyotype. Embryos that do not complete their first cleavage until 27 h after fertilization show a dramatically decreased development to diploid blastocysts (Figure 2), which defines this time point as a suitable cut-off to select for embryos with an abnormal karyotype (SUGIMURA et al., 2012).

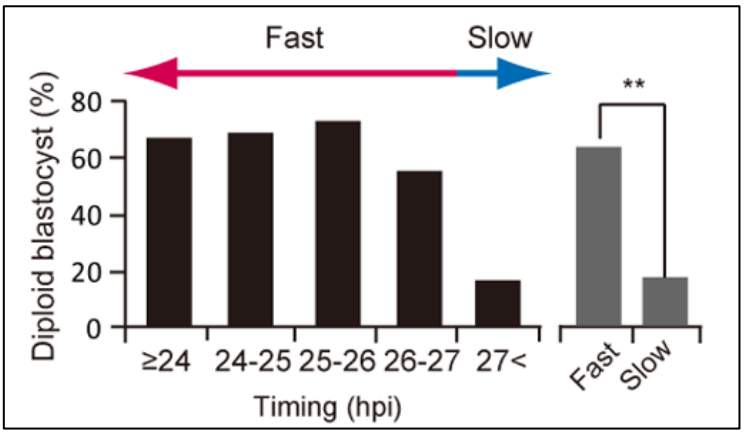

Figure 2: Relationship between timing of the first cleavage and the incidence of diploid embryos. Blastocysts were divided into two groups, fast and slow, based on the timing of the first cleavage with a cut-off of 27 hpi. Adapted from SUGIMURA et al. (2012).

A bovine chimeric embryo whose ICM solely contains cells derived from a donor embryo or a different source of pluripotent cells has not been reported yet, as the current strategies still fail to exclude the host from pluripotent lineages.

3. Use of phytohemagglutinin-L for embryo aggregation

Phytohemagglutinin-L (PHA) is the leukocyte specific subunit of a lectin produced from *Phaseolus vulgaris* (red kidney bean). It is a glycoprotein that binds to cellular surfaces by means of specific glycol conjugates and it has mitogenic and agglutinating properties (MINTZ et al., 1973; MALLIKARJUNAN et al., 2014).

When added to *in vitro* maturation medium of bovine oocytes or to embryo culture medium, it has no effect on embryonic development in low concentrations (WANG et al., 2001), but concentrations exceeding 300 µg/ml are detrimental (DU et al., 2006). The agent was also used in the SCNT procedure, where treatment of enucleated oocytes with PHA increased the fusion rate and overall efficiency or enabled performing the SCNT procedure without ZP or the use of a micromanipulation unit (VAJTA et al., 2001; OBACK et al., 2003; DU et al., 2006). PHA is a carbohydrate binding protein and therefore suitable to aggregate embryos, because embryos treated with PHA stick together and form stable constructs. First aggregation experiments were performed with mouse embryos, where firm and quick adhesion between aggregation partners already after short exposure was reported, which remained stable in PHA-free culture medium (MINTZ et al., 1973). With the aim to increase the efficiency of bovine SCNT, PHA was also successfully used to aggregate bovine embryos (MISICA-TURNER et al., 2007; AKAGI et al., 2011). To avoid uncontrolled aggregation after treatment with PHA, the constructs can be cultured in a well of the well (WoW) culture dish, which allows individual culture of aggregates while maintaining positive group culture effects (PALMA et al., 1992; VAJTA et al., 2000; FUJITA et al., 2006).

4. The pluripotency regulating transcription factor OCT4

The gene *OCT4* (*POU5F1*) encodes the octamer-binding transcription factor-4 (OCT4), which belongs to the pit-oct-unc (POU) family of transcription factors. It regulates the expression of candidate genes by binding through helix-turn-helix to an octamer sequence motif (ATGCAAAT) in their promoter and/or enhancer regions (SCHÖLER, 1991; HERR & CLEARY, 1995). *OCT4* is linked to the pluripotent properties of blastomeres, ESCs and iPSCs, where it maintains, induces and regulates pluripotency (WANG & DAI, 2010; WU & SCHÖLER, 2014). It is also required for the establishment of primordial germ cells (KEHLER et al., 2004). The OCT4 protein is highly conserved between species and mouse, human and bovine OCT4 are true orthologs with the bovine OCT4 sharing 90.6% and 81.7% identity with human and mouse OCT4, respectively (VAN EIJK et al., 1999).

4.1 *Oct4* in the preimplantation mouse embryo

In mouse embryos, the OCT4 protein is already found in oocytes and later it is located in all nuclei until blastocyst stage, when it is restricted to the nuclei in the ICM (PALMIERI et al., 1994). Exclusive expression of OCT4 in the ICM is established through downregulation of OCT4 in the TE by the TE-specific transcription factor CDX2 (NIWA et al., 2005; RALSTON & ROSSANT, 2008). It is now established, that *Oct4* is at the top of the pluripotency regulatory hierarchy (WU & SCHÖLER, 2014), although it is neither necessary for the first lineage segregation into ICM and TE nor for the initiation of toti- or pluripotency (NICHOLS et al., 1998; FRUM et al., 2013; WU et al., 2013).

These findings are based on KO studies, with the first being performed by NICHOLS et al. (1998), who found that *Oct4* KO mouse embryos develop until blastocyst stage, but without a pluripotent ICM and that the mutation results in peri-implantation lethality. Furthermore, the authors revealed that in the absence of OCT4, proliferation of the TE was not maintained, due to the missing fibroblast growth factor 4 (FGF4), which is a target gene of OCT4. Using a Cre/loxP recombinase system, it was possible to induce an *Oct4* KO in both the maturing oocytes and resulting zygotes. In short, Cre expression was driven from the *Zp3* promoter to induce recombination in the primary follicles' oocytes in females with a heterozygously floxed *Oct4*. Mating with heterozygous males resulted in progeny deficient of maternal and zygotic OCT4 at Mendelian frequencies. Studies employing this system found, that the establishment of totipotency is not OCT4 dependent, as embryos showed normal development until blastocyst stage (FRUM et al., 2013; WU et al., 2013; LE BIN et al., 2014). The first lineage differentiation in the embryo, when TE and ICM segregate, is not compromised by an *Oct4* KO. At day 3.5 (the late blastocyst stage), *Oct4* KO embryos exhibit normal cell numbers in the TE and ICM and also expression of GATA3 and CDX2, factors that induce differentiation of the TE, are repressed in the ICM (NICHOLS et al., 1998; RALSTON et al., 2010; WU et al., 2013).

The second lineage differentiation begins at the late blastocyst stage, when epiblast (EPI) and primitive endoderm (PE) segregate within the ICM. Precursor cells already

express lineage specific marker genes, resulting in a salt and pepper distribution of NANOG and GATA6 positive blastomeres, which later form EPI and PE by day 3.75, respectively (CHAZAUD & YAMANAKA, 2016). Embryos deficient of OCT4 also exhibit a mutually exclusive expression of NANOG and GATA6 at day 3.75. With ongoing development, GATA6 positive cells disappear from the ICM and the proportion of cells neither expressing GATA6 nor NANOG (unlabeled cells) increases until day 4.25, when almost no GATA6 positive cells are found. Activation of PE specific gene expression, i.e. *Gata6, Sox17* and *Sox7,* fails and thus there is no development of PE (FRUM et al., 2013; LE BIN et al., 2014).

In mouse embryos, expression of PE genes can be induced by addition of exogenous FGF4 and heparin (FGF4/hep) to the culture medium, with the result that all cells of the ICM will express GATA6 (YAMANAKA et al., 2010). Additionally, embryos lacking FGF4 have an ICM entirely made up of NANOG positive cells (KANG et al., 2013) and the same is also true for embryos treated with FGFR/MAPK signaling inhibitors (LANNER & ROSSANT, 2010). *Fgf4* is a target gene of OCT4 and *Fgf4* mRNA levels in *Oct4* KO embryos are reduced (NICHOLS et al., 1998). Treatment of *Oct4* KO embryos with FGF4/hep cannot activate PE gene expression or repress NANOG expression, leading to the conclusion that OCT4 is required for exogenous FGF4 to act upon cells in the ICM. In chimeras from an *Oct4* KO embryo and wild-type ESCs, the ESCs are not able to rescue PE development, so OCT4 is required cell-autonomously for PE differentiation (FRUM et al., 2013; LE BIN et al., 2014). In summary, the current working model (Figure 3) states, that in EPI cells OCT4 regulates the expression of FGF4, which induces PE cell fate and that additionally, OCT4 in the PE cells activates the expression of PE genes (FRUM et al., 2013).

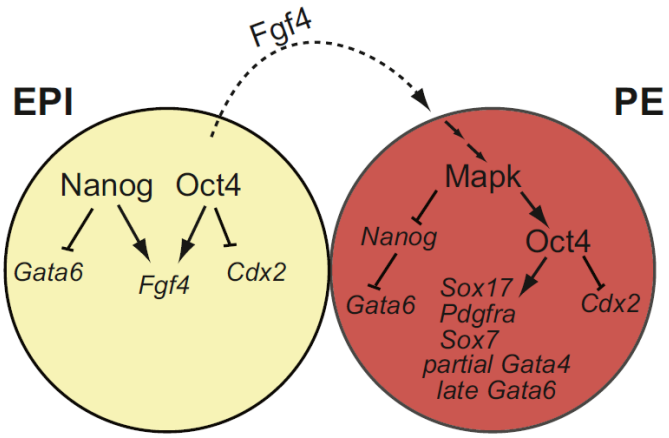

Figure 3: Working model of OCT4 during the second lineage differentiation. Adapted from FRUM et al. (2013).

4.2 *OCT4* in the preimplantation bovine embryo

Bovine embryos develop to early blastocysts at day 6-7 and segregation of EPI and hypoblast (HB, the equivalent to the PE in mouse) in the ICM occurs around day 8 (MADDOX-HYTTEL et al., 2003), while implantation begins at day 16-18 (HYTTEL et al., 2009). Mouse embryos develop at a faster pace, reaching implantation already at day 4.5 (NAGY et al., 2003). Similar to mouse embryos, maternal *OCT4* transcripts are already detected in the oocyte and decrease until the 8-16 cell stage, when embryonic genome activation (EGA) occurs. After EGA, OCT4 is detected in all nuclei of the morula (KIRCHHOF et al., 2000; KUROSAKA et al., 2004; WUENSCH et al., 2007). While the canonical lineage marker CDX2 extinguishes OCT4 expression in the TE of day 3.5 late mouse blastocysts, bovine embryos co-express CDX2 and OCT4 in the TE until day 11. Mouse CDX2 is able to shut down OCT4 expression due to the conserved region 4 (CR4) in the *Oct4* locus, which differs from the bovine and human CR4. When the mouse CR4 is exchanged with the bovine, CDX2 no longer extinguishes OCT4 expression in mouse TE. This difference in mouse preimplantation development to other species allows rapid differentiation of the TE and implantation of the embryo (NORDHOFF et al., 2001; BERG et al., 2011).

At day 8, the same salt and pepper distribution of GATA6 and NANOG positive cells is present in the bovine ICM when compared to the mouse. Nevertheless, the role of FGF4 is not analog to the situation in the mouse: inhibition of MAPK, FGFR or FGF4 signaling only partially blocks GATA6 expression and therefore HB development in the bovine embryo, while addition of FGF4/hep leads to GATA6 expression in all ICM cells. Therefore, FGF signaling is not required for normal GATA6 expression and the effect of exogenous FGF4 on GATA6 expression is indirect in bovine embryos (KUIJK et al., 2012).

At the time of writing this review, no knockout study but two knockdown studies of *OCT4* had been performed in bovine embryos, which used RNA interference to suppress transcription of *OCT4*. NGANVONGPANIT et al. (2006) reported successful reduction of *OCT4* transcript abundance by 72% at blastocyst stage, but development to day 5 morulae or total blastocyst rate remained unchanged. Reduction of *OCT4* concomitantly reduced the level of *FGF4* transcripts, showing that - like in mouse - FGF4 is regulated by OCT4. The authors also recorded a reduced cell number in the ICM of *OCT4* knockdown blastocysts, while the number of TE cells did not differ. More recently, SAKURAI et al. (2016) followed the same methodological approach and confirmed the dependence of FGF4 on OCT4. Nevertheless, they recorded a reduced blastocyst rate and *OCT4* knockdown day 7 blastocysts had only half as much total cells as controls. Existing data on the function of OCT4 in bovine embryos is scarce and in part contradicting. Additionally, differences in OCT4-CDX2 interaction and in regulation of GATA6 expression through FGF4 signaling between bovine and mouse suggest, that the underlying mechanisms involving OCT4 are not the same and that the model organism mouse does not entirely reflect the early developmental events in bovine embryos. Therefore, it is necessary to study the role of OCT4 in bovine embryos with a definitive knockout.

5. CRISPR/Cas9

Genome editing tools, i.e. zinc-finger nucleases (ZFN), transcription activator-like effector nucleases (TALEN) and Cas9 endonuclease associated to clustered regulatory interspaced palindromic repeats (CRISPR/Cas9), enable researchers to

manipulate any gene in a broad range of organisms. These tools are capable of inducing a double strand break (DSB) at a defined location, which leads to DNA repair mechanisms, amongst others non-homologous end-joining repair (NHEJ) and homology directed repair (HDR). The error prone NHEJ eventually leads to insertions or deletions (indels) of nucleotides, while through HDR a perfect repair of the DSB or targeted insertion of an exogenous repair template may be achieved (GAJ et al., 2013). The CRISPR/Cas9 system is derived from an ancient bacterial defense mechanism, where CRISPRs represent the memory from previous infections and the Cas9 endonuclease the effector inducing the DSB in foreign DNA (SERUGGIA & MONTOLIU, 2014). In bacteria, the CRISPRs are processed into CRISPR RNAs (crRNAs), which bind to trans-activating RNAs (tracrRNA) to form a complex with Cas9. To use CRISPR/Cas9 as a genome editing tool, the fusion product of the crRNA and tracrRNA (gRNA) is introduced to a cell or organism together with Cas9. 20 customizable nucleotides at the 5' end of the gRNA, the small guiding RNA (sgRNA), then direct Cas9 to a specific site through Watson&Crick base pairing, where Cas9 finally induces a DSB. The only limitation in designing the sgRNA is the obligatory presence of a NGG protospacer adjacent motif (PAM) at its 3' end, which on average occurs every 8 bp in the mammalian genome (SANDER & JOUNG, 2014; SERUGGIA & MONTOLIU, 2014). In comparison with ZFNs and TALENs, CRISPR/Cas9 is easier to design, has a higher mutagenesis efficiency and is inexpensive (SERUGGIA & MONTOLIU, 2014). Also, it enables simultaneous multiplex editing of several genes (HSU et al., 2014).

The first application report of CRISPR/Cas9 in mammalian embryos was published by WANG et al. (2013), who simultaneously disrupted five genes in mouse ESCs, which can be used to produce offspring with germline transmission. They also generated mice with a biallelic knockout of two genes by injection of CRISPR/Cas9 to the cytoplasm of zygotes, which allowed the production of mutant mice in only one step with a very high efficiency of 80%. Subsequently, this approach was repeated targeting a single gene in pig zygotes, which resulted in 37.5% of the offspring carrying a biallelic mutation (HAI et al., 2014). Bovine zygotes and iPSCs were also targeted with CRISPR/Cas9 to achieve a gene knockin with an efficiency of 14% in blastocysts and 100% in picked colonies (HEO et al., 2014). In sheep, KO

of the myostatin gene (*MSTN*), a desired mutation in livestock species, was achieved by injection of CRISPR/Cas9 to zygotes, with 36.4% of the offspring carrying a biallelic mutation (CRISPO et al., 2015). A disadvantage in generation of genome-edited animals through injection of CRISPR/Cas9 at the zygote stage is the occurrence of mosaicism in the offspring. A study that targeted the *Tyr* locus in mouse zygotes (a knockout results in complete albinism) reports, that from 33 pups one complete albino and three pigmentation mosaics were generated while the rest was fully pigmented. Deep sequencing also showed, that the majority of the mutated pups had more than two new mutant alleles (YEN et al., 2014). Also in pig, mosaic offspring has been reported after zygote injection (WHITWORTH et al., 2014) and at a high frequency of 80% also in sheep (CRISPO et al., 2015). Somatic mosaicism and allele complexity may complicate subsequent work, especially when the mosaicism also affects the germline (YEN et al., 2014). A common strategy to produce genetically modified animals, mainly in species where ESCs don't exist, is to target somatic cells and reconstruct embryos via SCNT. With this approach, mosaicism is unlikely to occur and the exact mutation is known before transfer of embryos to recipients. With this strategy, goats with a *MSTN* KO and pigs with a KO of *CD163* and *CD1D* were successfully produced (NI et al., 2014; WHITWORTH et al., 2014). Bovine fibroblasts were also transfected to produce a knockin of human *FGF2* at the β-casein gene locus with subsequent embryo production through SCNT (JEONG et al., 2016), but still there is no report on bovine CRISPR/Cas9 genome-edited offspring, neither through zygote injection nor SCNT.

CRISPR/Cas9 technology bares great possibilities for the study of preimplantation embryonic development, because the function of genes may be easily determined, e.g. by performing KO or knockin of a reporter construct. Using these new strategies, i.e. injection at the zygote stage or reconstruction with modified somatic cells, investigators are now able to verify, if mechanisms established in the mouse model proof true for other mammalian species. A first report is available in the pig, where a *OCT4* KO was successfully induced by CRISPR/Cas9 injection at the zygote stage (KWON et al., 2014) and in the United Kingdom, researches gained the permit to investigate the role of *OCT4* in human embryos using CRISPR/Cas9 (CALLAWAY, 2016).

The aims of this thesis were i) to study the feasibility of multiplying selected bovine embryos by aggregation with host embryos and ii) to investigate the role of OCT4 in bovine preimplantation embryos including the implications on the second lineage differentiation.

Multiplication of selected embryos was studied by aggregating pairs of blastomeres from day 5 morulae with two day 4 host embryos, which did not complete their first cleavage until 27 h after *in vitro* fertilization (IVF). Also, the effect of PHA on chimera formation and position of the donor cells in the chimeric blastocysts was investigated.

To investigate the role of OCT4, a KO model was established, which allowed the production of *OCT4* KO embryos with SCNT using mutated donor nuclei. The *OCT4* KO phenotype was then analyzed by immunofluorescence staining of the markers of all three lineages in the preimplantation embryo, i.e. CDX2, GATA6 and NANOG for the TE, HB and EPI, respectively. With data from confocal laser scanning microscopy (CLSM), it was possible to thoroughly analyze the impact of OCT4 deficiency on embryonic development.

Additionally, aggregation of wild-type embryos with embryos lacking a pluripotent lineage (*OCT4* KO embryos) was performed to test the biotechnological use of *OCT4* KO embryos in multiplication of elite embryos and to investigate, if few wild-type blastomeres can rescue the lethal *OCT4* KO phenotype.

III. Materials and Methods

1. Materials

1.1 Apparatuses

170-300 incubator	MMM Group, Munich
5µl Transferpettor glass pipet	Brand, Wertheim
5415 D centrifuge	Eppendorf, Hamburg
5417 R centrifuge	Eppendorf, Hamburg
5810 R centrifuge	Eppendorf, Hamburg
9040-0071 incubator	Binder, Tuttlingen
Accu-jet® pro pipette controller	Brand, Wertheim
Agarose gel electrophoresis chamber	WG - Biotech, Ebersberg and OWL Inc., USA
Axiovert 200 M epifluorescence microscope	Zeiss, Oberkochen
Biofuge pico centrifuge	Heraeus, Osterode
Cellavista	SynenTec, Münster
CO_2Cell incubator	MMM Group, Munich
CoolCell	BioCision, USA
EASYpure® II	pure aqua, Schnaitsee
EBA 8S centrifuge	Hettich, Tuttlingen
Gel documentation system	BioRad, Munich
Geneamp PCR System 9700 thermocycler	Applied Biosystems, USA
GeneQuant Pro spectrophotometer	Thermo Scientific, Schwerten

HAT 200 warming plate and heated microscope stage	Minitube, Tiefenbach
Labcycler thermocycler	SensoQuest, Göttingen
Laminar flow HB 2448K	Heraeus, Hanau
Laminar flow HeraSafe HS12	Kendro, Hanau
Laminar flow HV228	K Systems, Denmark
LSM 710 confocal laser scanning microscope	Zeiss, Oberkochen
Microwave	DAEWOO, Korea
MS 5 Stereomicroscope	Leica, Wetzlar
Neubauer counting chamber	Hecht Assistent, Sondheim vor der Rhön
Nucleofector™ II	Lonza, Switzerland
Pipettes (1000 µl, 200 µl, 10 µl)	Brand, Wertheim
Pipettes (1000 µl, 200 µl, 100 µl, 20 µl, 10 µl, 2.5 µl)	Eppendorf, Hamburg
Pipettes (1000 µl, 200 µl, 20 µl, 2 µl)	Gilson Inc, USA
Power Pac 300 gel electrophoresis unit	BioRad, Munich
Power Station 300 gel electrophoresis unit	Labnet International, USA
Rotanda 96 centrifuge	Hettich, Tuttlingen
Select vortexer	Select BioProducts, USA
Spectrafuge 24 D centrifuge	Labnet International, USA
SZ11 stereomicroscope	Olympus, Japan

1.2 Software

AxioVision V 4.9.1.0	Zeiss, Oberkochen
Bio Edit Sequence Alignment Editor	Tom Hall, USA

Fiji image J distribution	National Institutes of Health, USA
Finch TV Version 1.3.1	Geospiza Inc., USA
Icy 1.6.0.0	Institut Pasteur, France
Microsoft Office Suite	Microsoft, USA
Prism 5.02 for Windows	GraphPad Software, USA
Zen 2012 SP1 (black edition)	Zeiss, Oberkochen

1.3 Consumables

0.22 µm sterile filter	Merck Millipore, Darmstadt
100 mm culture dish	Sarstedt, Nümbrecht
Primovision embryo culture dish	Vitrolife, Sweden
24-well culture plate	Nunclon delta surface, USA
30 mm cell culture dish	Nunc, Braunschweig
48-well culture plate	Nunclon delta surface, USA
4-Well culture plate	Nunc, Braunschweig
60 mm culture dish	Sarstedt, Nümbrecht
6-well culture plate	Cellstar Greiner Bio One, Frickenhausen
96-well culture plate	Nunclon delta surface, USA
96-well half area 3696 culture plate	Corning Costar, USA
Centrifuge tubes (10 ml)	Nunc, Braunschweig

Centrifuge tubes (15 ml, 50 ml)	Falcon, Becton Dickinson, Heidelberg
Coverslips (26 x 21 mm, 0.17 ± 0.01 mm)	Hecht Assistent, Sondheim vor der Rhön
Coverslips (76 x 26 mm, 0.17 ± 0.01 mm)	Hecht Assistent, Sondheim vor der Rhön
Cryo vial (0.5 ml, 1.5 ml)	TPP, Switzerland
Glass pasteur pipettes	Brand, Wertheim
PCR reaction tubes (0.2 ml)	Brand, Wertheim
Perforated adhesive-backed PVC-film	Mactac, USA
Pipet tips with filter (10 µl, 20 µl, 200 µl, 1000 µl)	Kisker Biotech, Steinfurt
Pipette tips (250 µl, 1000 µl)	Eppendorf, Hamburg
Safe-Lock reaction tubes (0.5 ml, 1.5 ml, 2 ml)	Eppendorf, Hamburg
Sperm, sire Mirsanmir	Bayern Genetik, Grub

1.4 Chemicals , enzymes and other reagents

1,4-Dithiothreitol (DTT)	Sigma, Steinheim
2-Mercaptoethanol	Roth, Karlsruhe
Albumin, from bovine serum	Sigma, Steinheim
Amaxa™ Basic Nucleofector™ Kit Primary Fibroblasts	Lonza, Switzerland
Aprotinin from bovine lung	Sigma, Steinheim
BigDye® Terminator v3.1	Applied Biosystems, Weiterstadt
BME amino acids solution	Sigma, Steinheim
Bromophenolblue	Merck, Darmstadt
$CaCl_2H_2O$	Sigma, Steinheim

Chloroform (Trichloromethane)	Roth, Karlsruhe
Deuteriumoxid	Fisher Scientific, USA
Donkey serum	Jackson Immuno Research, United Kingdom
dNTPs (dATP, dCTP, dGTP, dTTP)	Thermo Scientific, Schwerte
EDTA (Ethylenediaminetetraacetic acid)	Roth, Karlsruhe
EGTA (Ethylene glycol-bis(β-aminoethyl ether)-N,N,N′,N′-tetraacetic acid tetrasodium salt)	Sigma, Steinheim
Ethanol	Roth, Karlsruhe
Ethidiumbromide (1mg/mL)	Merck, Darmstadt
Fetal calf serum	Invitrogen, Karlsruhe
Gene Ruler^{TM} 1 kb	Thermo Scientific, Schwerte
Glycerin (Glycerol)	Roth, Karlsruhe
Heparin	Sigma, Steinheim
HEPES	Sigma, Steinheim
Herculase II Fusion DNA Polymerase	Agilant technologies, USA
Herculase II 5x reaction buffer	Agilant technologies, USA
Isopropanol	Roth, Karlsruhe
KCl	Sigma, Steinheim
MEM Non-essential amino acid solution	Sigma, Steinheim
$Mg_2Cl_2H_2O$	Sigma, Steinheim

$MgCl_2$	Fluka Chemie, Switzerland
Na lactate sirup (60%)	Sigma, Steinheim
NaCl	Sigma, Steinheim
$NaH_2PO_2H_2O$	Sigma, Steinheim
$NaH_2PO_4H_2O$	Sigma, Steinheim
$NaHCO_3$	Sigma, Steinheim
Estrous cow serum (OCS)	In house production
Paraformaldehyde	Sigma, Steinheim
Phenol red	Sigma, Steinheim
Phytohaemagglutinin (PHA)	Sigma, Steinheim
Pipes	Sigma, Steinheim
Polyvinylalcohol (PVA)	Sigma, Steinheim
Pronase	Sigma, Steinheim
Proteinase K, ready to use	Dako, Hamburg
Pyruvic acid	Sigma, Steinheim
SDS (Sodium dodecyl sulfate)	Serva Electrophoresis, Heidelberg
Sodium acetate	Sigma, Steinheim
Taxol	Sigma, Steinheim
Tris (Tris-(hydroxymethyl)-aminomethane)	Roth, Karlsruhe
Triton X-100	Sigma, Steinheim
Universal Agarose	Bio&SELL, Nürnberg
Vectashield with DAPI	Vector Laboratrories, USA

1.5 Oligonucleotides

OCT4 2f	5‘-TTGTGGGACCTTCAAAGTAATC-3‘
OCT4 2r	5‘-CTGCAGATTCTCGTTGTTGT-3‘
OCT4 12f	5‘-TATGTTCTTACATATCCTCTGC-3‘
OCT4 11f	5‘-CTCTTTGGTGAGTCTCCTACAG-3‘
ETF1 2f	5‘-TTGGGTGTGAAGTGGGTTTG-3‘
ETF1 2r	5’-CTGGGCGATGTGGCTAATTT-3’
ETF1 3f	5’-CTATGACTTGTGTGGAGGGATG-3’
boOCT4 sgRNA	5‘-GATCACACTAGGATATACCCAGG-3‘

1.6 Antibodies

Rabbit anti-human NANOG 500-P236	Peprotech, Hamburg
Goat anti-human GATA6 AF1700	R&D Systems, USA
Rabbit anti-human CDX2 ab88129	Abcam, United Kingdom
Goat anti-human OCT4 SC8628	Santa Cruz Biotechnology, USA
Donkey anti-rabbit Alexa Fluor 555 ab150074	Abcam, United Kingdom
Donkey anti-goat Alexa Fluor 633 A212082	ThermoFisher, USA

1.7 Hormones

Follicle stimulating Hormone (FSH) 50 Units	Sioux Biochemical, USA
Luteinizing Hormone (LH) 25 Units	Sioux Biochemical, USA

1.8 Media and Buffers

1.8.1 Buffers

Water deionized in a Millipore device (EASYpure® II) was used as solvent.

Phosphate buffered saline (PBS)

NaCl	8	mg/ml
KCl	0.2	mg/ml
KH_2PO_4	0.2	mg/ml
$NaH_2PO_4 \cdot H_2O$	1.15	mg/ml
$MgCl_2 \cdot H_2O$	0.1	mg/ml
$CaCl_2$	0.1	mg/ml

PBS without $MgCl_2$ and $CaCl_2$ (PBS w/o Mg^{2+}, Ca^{2+})

NaCl	8	mg/ml
KCl	0.2	mg/ml
KH_2PO_4	0.2	mg/ml
$NaH_2PO_4 \cdot H_2O$	2.14	mg/ml

PK-Buffer

Tris	200	mM
NaCl	1	M
EDTA	40	mM

T-Buffer

Tris	10	mM

TE-Buffer

Tris	10	mM
EDTA	1	mM

TAE-Buffer

Tris	2	M
EDTA	50	mM

1.8.2 Media for in vitro production of embryos

Stocks

Pyruvate stock	2,2 mg/ml pyruvic acid in 0.9% NaCl solution
Heparin stock	0.5 mg/ml heparin in Fert Talp stock
Gentamycin stock	50 mg/ml gentamycin sulfate in 0.9% NaCl solution
L-gluthamine stock	200 mM in ddH_2O
FSH stock	5 Units/ml in 0.9% NaCl
LH stock	2.5 Units/ml in 0.9% NaCl

Maturation medium (Modified Parker's Medium, MPM)

Solution 1:

Calcium L-lactate hydrate in ddH_2O	6	mg/ml

Soultion 2:

$NaHCO_3$	3	mg/ml
HEPES	1.4	mg/ml
Pyruvat	0.25	mg/ml
Gentamycin-Stock µl	1.1	mg/ml
TCM 199 10x (Life Technologies)	100	µl/ml

Maturation medium (MPM):

Solution 1 + solution 2	1+10

Supplementation (10 ml):

FSH stock	50	µl (=0.025 U/ml)
LH stock	50	µl (=0.0125 U/ml)
OCS	500	µl

Medium for *in vitro* fertilization (Fert Talp)

NaCl	6.66	mg/ml
KCl	0.235	mg/ml
$NaHCO_3$	2.103	mg/ml
$NaH_2PO_4H_2O$	0.047	mg/ml
Penicilline	0.065	mg/ml
Phenol red	0.01	mg/ml
Na lactate sirup (1.3 g/ml)	1.86	µl/ml
$MgCl_2H_2O$	0.1	mg/ml
$CaCl_2H_2O$	0.397	mg/ml

Supplementation (10 ml):

Bovine serum albumin	60	mg
Pyruvate stock	100	µl
Heparin stock	300	µl

Medium for sperm capacitation (Sperm Talp)

NaCl	5.8	mg/ml
$NaHCO_3$	2.09	mg/ml
$NaH_2PO_2H_2O$	0.04	mg/ml
HEPES	2.38	mg/ml
$MgCl_2H_2O$	0.31	mg/ml
$CaCl_2H_2O$	0.384	mg/ml

Phenol red	0.01	mg/ml
Na lactate sirup (1.3 g/ml)	3.65	µl/ml
Supplementation (10 ml):		
Bovine serum albumin	60	mg
Pyruvate stock	500	µl

Medium for *in vitro* culture (synthetic oviduct fluid, SOF)

NaCl	62.92	mg/ml
KCl	0.53	mg/ml
KH_2PO_4	0.162	mg/ml
$CaCl_2H_2O$	0.248	mg/ml
$MgCl_2H_2O$	0.096	mg/ml
NaHCO3	2.106	mg/ml
Phenol red	0.0014	mg/ml
Pyruvate	0.363	mg/ml
L-gluthamine stock	5	µl/ml
Na lactate sirup (1.3 g/ml)	0.47	µl/ml
Supplementation (10 ml):		
BME Amino acid solution	400	µl
MEM Amino acid solution	100	µl
OCS	500	µl

1.8.3 Media for embryo manipulation and fixation

HEPES-buffered Tyrode's medium with 0.1% PVA (TL-HEPES-PVA)

NaCl	6.65	mg/ml
KCl	0.24	mg/ml
$NaHCO_3$	0.17	mg/ml
NaH_2PO_4	0.04	mg/ml
Sodium lactate	1.12	mg/ml
$CaCl_2$	0.22	mg/ml
$MgCl_2$	0.05	mg/ml
HEPES	2.38	mg/ml
Phenol red	0.01	mg/ml
Glucose	0.9	mg/ml
Sorbitol	8	mg/ml
Stroptomycin sulfate	0.05	mg/ml
Penicillin-G	0.065	mg/ml

Protease in PBS

Protease P5147	5	mg/ml
PVA	1	mg/ml

Albertini-solution for fixation of embryos

Pipes (0.5 M)	200	µl
$MgCl_2$ (50 mM)	100	µl
EGTA (50 mM)	50	µl
Deuteriumoxid	445	µl
Paraformaldehyde (10%)	200	µl
Triton X-100	5	µl

Aprotinin	1	µl
Taxol (5 mM)	0.2	µl
Total volume	1001.2	µl

1.8.4 Media for cell culture

Culture medium

DMEM (1x) + GlutaMAX (GIBCO by life technologies) supplemented with

Non-essential amino acids (100 ×)	1	%
β-mercaptoethanol	0.1	mM
Fetal calf serum (FCS)	10 - 15	%

Stop medium

DMEM (1x) + GlutaMAX (GIBCO by life technologies) supplemented with

FCS	10	%

Starvation medium

DMEM (1x) + GlutaMAX (GIBCO by life technologies) supplemented with

Non-essential amino acids (100 ×)	1	%
FCS	0.5	%

Cryo medium

FCS + DMSO 9+1

Tryspin/EDTA

0.5% Trypsin + 0.04% EDTA in PBS w/o Mg^{2+}, Ca^{2+}

2. Methods

2.1 *In vitro* production of bovine embryos

All embryos were produced *in vitro* according to a standard procedure including *in vitro* maturation (IVM) and *in vitro* fertilization (IVF) (HIENDLEDER et al., 2004). Ovaries were collected in PBS pre-warmed to 36° C at the local abattoir. Follicles with a diameter of 2-8 mm were aspirated with a vacuum pump set to 80-100 mmHg and after washing three times, obtained cumulus–oocyte complexes (COCs) were matured for 23 h in groups of 40 in 10 µl maturation medium per COC. Frozen-thawed sperm of a bull with proven fertility was thawed for 10 sec in a 38° C warm water bath and prepared by the swim-up method. Four 10 ml tubes were filled with each 1 ml Sperm Talp medium and 50 µl of sperm were layered underneath. Tubes were incubated at 39° C and after 1 h, the upper layer of the tubes was collected and centrifuged at 500 rcf. The supernatant was removed and concentration was determined using a Neubauer improved counting chamber. Matured COCs were transferred to Fert Talp medium and co-incubated with $1x10^6$ sperm/ml. For IVM and IVF, COCs were incubated at 39° C in a maximum humidified atmosphere of 5% CO_2 in air. After 20 h of co-incubation, presumptive zygotes were vortexed for 3 min to remove remaining cumulus cells and washed three times. Zygotes with no remaining cumulus cells were cultured in groups of 40 in 400 µl of synthetic oviductal fluid (SOF) under 400 µl mineral oil at 39° C in a maximum humidified atmosphere of 5% CO_2, 5% O_2, and 90% N_2.

2.2 Embryo manipulation

All embryo manipulations were performed on a heated microscope plate set to 36° C. Where not indicated differently, embryos were transferred to drops of TL-HEPES-PVA for handling outside the incubator (KUROME et al., 2015).

2.3 *Zona pellucida* removal

On Day 4, 5 or 7 of embryonic development, the ZP was removed by treatment with 5 mg/ml of protease for 1 minute. Enzyme reaction was stopped by washing embryos in TL-HEPES-PVA supplemented with 10% fetal calf serum. Dissolved ZP was

completely removed by gentle pipetting with a finely drawn glass pipet with sharp ends and an inner diameter of 80 µm.

2.4 Morula disaggregation

To disaggregate morulae after ZP removal, they were incubated for 20 min in drops of PBS w/o Mg^{2+}, Ca^{2+} supplemented with 0.1% PVA under oil on a heated microscope stage set to 36° C. Through pipetting with a blunt glass pipet with an inner diameter of 80 µm, blastomeres were completely individualized.

2.5 Chimera production

Chimeras were produced from two ZP-free day 4 host embryos (~16 cells) that did not complete their first cleavage until 27 h after IVF and two blastomeres from a day 5 eGFP transgenic embryo (donor), produced by using semen from an eGFP transgenic bull for IVF (REICHENBACH et al., 2010). Alternatively, chimeras were produced from two day 4 *OCT4* knockout (KO) host embryos derived from *WalterBF-Tg(PGK-EGFP)POU5F1*^{1AH1tm1} fibroblasts and four blastomeres of a day 4 wild-type *in vitro* produced embryo. The chimera production scheme is shown in Figure 4.

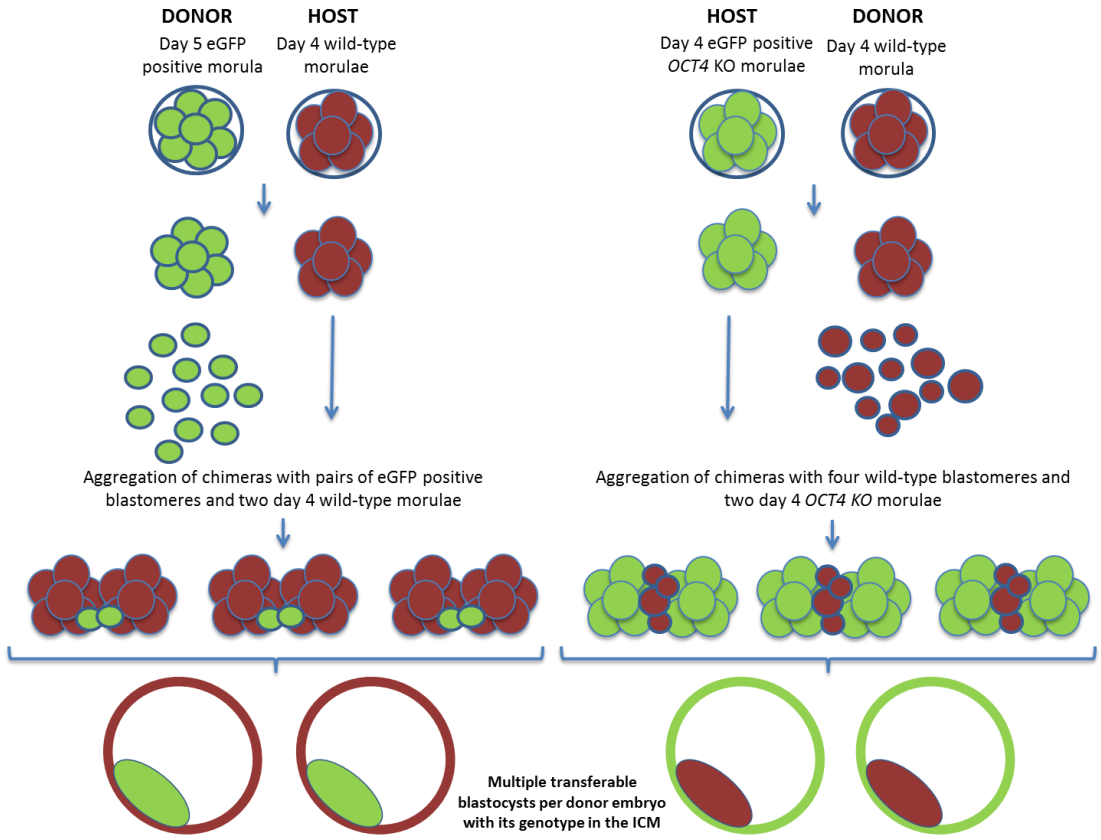

Figure 4: Chimera production scheme

2.5.1 Sandwich technique

In the sandwich technique, first a host embryo was transferred to a depression of a 4x4 WoW culture dish (Primovision embryo culture dish) with 160 µl SOF covered by mineral oil. Subsequently, the donor blastomeres were added and topped by the second host embryo to ensure close contact of the chimera's constituents and to position the donor blastomeres in between the hosts (BERG et al., 2011).

2.5.2 Aggregation technique

Host embryos were washed in SOF and transferred in pairs to drops of SOF supplemented with 150 µg/ml PHA and incubated for 20 min under embryo culture conditions. After incubation, pairs of blastomeres from the donor embryo were added to the drops and pushed in between the two host embryos with a closed and finely drawn pipet, so the blastomeres stuck firmly to the host embryos. Stable constructs were subsequently washed in SOF and transferred individually into the depressions of a WoW culture dish. The aggregation technique is shown in Figure 5.

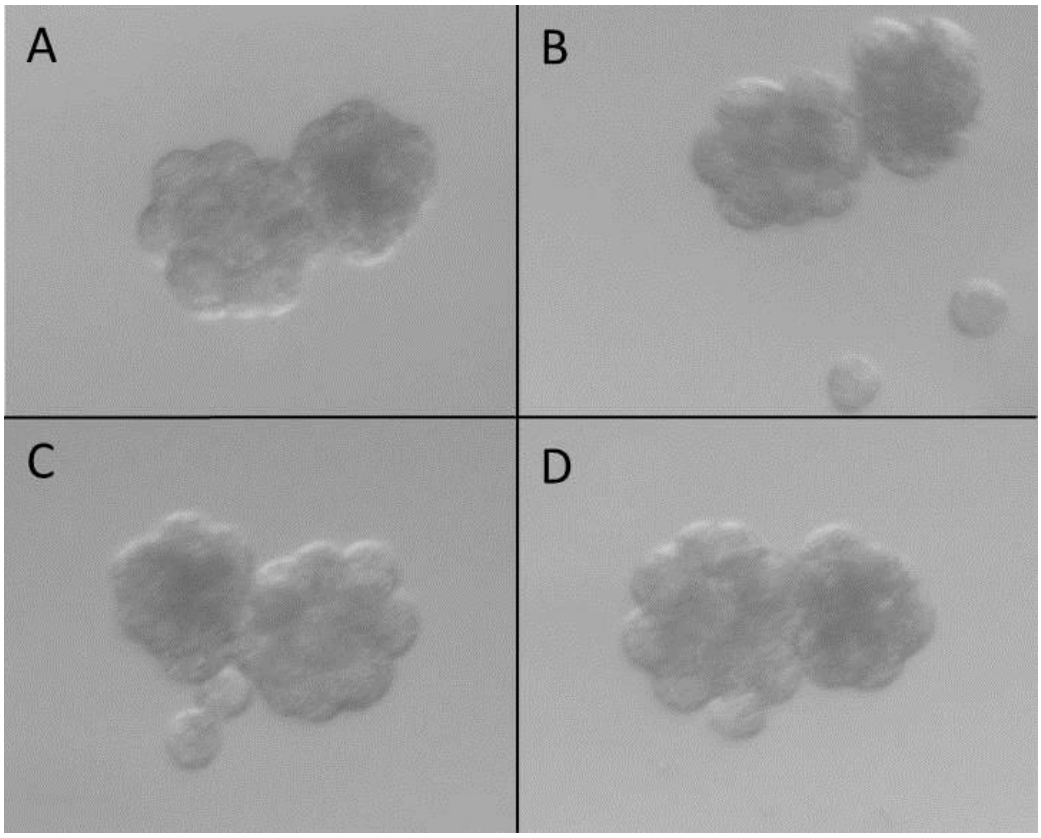

Figure 5: Aggregation of two day 4 host embryos and two day 5 donor blastomeres using PHA. A: two host embryos stuck together after incubation in SOF + PHA for 20 min. B: two donor blastomeres added to the drop. C: after sticking the donor blastomeres together, they are positioned in between host embryos. D: donor blastomeres are pushed firmly against host embryos. Adapted from SIMMET et al. (2015a).

2.6 Time lapse imaging

To compare the development of chimeras produced by the different techniques, WoW culture dishes were placed into the Primo Vision embryo monitoring system (Vitrolife, Gothenburg, Sweden). Images were recorded every 5 min for 96 h.

2.7 Cell culture procedures

All solutions and media were prewarmed to 37° C before use, unless indicated otherwise. Cells were incubated at 38.5° C in a maximum humidified atmosphere with 5% CO_2 in air and centrifuged at 500 rcf for 5 min. Previously isolated bovine fibroblast cells from an eGFP transgenic bull (*WalterBF-Tg(PGK-EGFP)*) were thawed at room temperature by adding Stop medium to the cryo vial. Cells were transferred to an adequate tube and centrifuged. The pellet was resuspended in culture medium and cells were seeded on plates appropriate to the amount of cells

(1.4 - 1.6 cells/cm^2). To harvest the cells after attachment to the culture dish, cells were washed twice with PBS w/o Mg^{2+}, Ca^{2+} and after adding trypsin/EDTA solution incubated for 3 min. Trypsin reaction was stopped with Stop medium and cells were centrifuged for further processing. To freeze cells, the pellet was resuspended with Cryo medium cooled to 4° C and transferred to a cryo vial, which was cooled slowly in a CoolCell device (BioCision) over night at -80° C before storage in liquid nitrogen (LN_2).

2.8 CRISPR/Cas9 mediated production of *OCT4* knockout host embryos

2.8.1 CRISPR/Cas9 design

To knock out the *OCT4* gene in bovine adult fibroblast cells, a CRISPR/Cas9 system was employed. A sgRNA was designed to bind at exon 2 of the *OCT4* gene (Figure 6) using chopchop software (MONTAGUE et al., 2014). The construct expressing the fusion of the sgRNA and tracrRNA, as well as a construct expressing Cas9 according to MALI et al. (2013) was purchased from Life Technologies, Invitrogen.

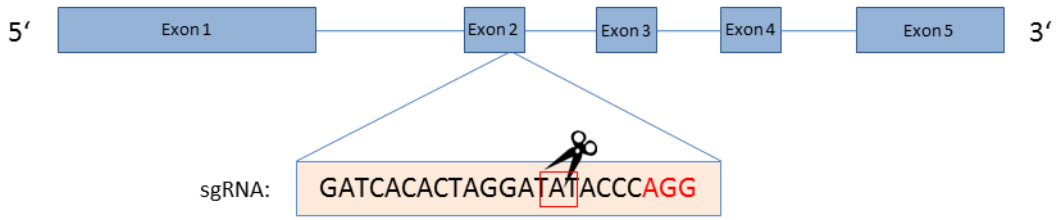

Figure 6: OCT4 gene, sgRNA and Cas9 cutting site 6 bp upstream from the protospacer adjacent motif (PAM, red letters).

2.8.2 Transfection of adult fibroblasts

Transfection of adult fibroblasts was performed with the Nucleofector™ device and the Amaxa™ Basic Nucleofector™ Kit for primary fibroblasts including Basic Nucleofector™ solution, cuvettes and Pasteur pipets. 1x10^6 eGFP transgenic cells from *WalterBF-Tg(PGK-EGFP)* were seeded on a 10 mm culture dish and cultured for 24 h to obtain mainly mitotic cells. Subsequently, 0.5x10^6 cells were resuspended

with Basic Nucleofector™ solution at room temperature and each 1 µg of CRISPR and Cas9 plasmid was added to the suspension, which was then transferred to the cuvette. Transfection was performed using the predefined program U12 from the Nucleofector™ device and the suspension was added to culture medium, equilibrated in a well of a 6-well plate, using the Pasteur pipet included in the kit. 24 h after transfection, the culture medium was renewed.

2.8.3 Selection of single cell clones

To produce single cell clones, each 100 cells from the previous transfection were seeded on 10x 96-well half area plates and culture medium was exchanged every three days. Five days after seeding, plates were scanned daily for single cell clones using Cellavista (Synentec), a fully automated cell imaging device that photographs each well and stores the pictures so development and integrity of single cell clones is documented. At 80% confluence, single cell clones were harvested and split on two wells of 96-well plates. When full confluence was reached, cells of one well were cryopreserved as backup and cells from the second well were used for DNA isolation to screen for mutations.

2.8.4 DNA isolation

DNA isolation from fibroblast cells was achieved through precipitation of DNA in a solution with a high salt concentration. After centrifugation, the cell pellet was resuspended with 100 µl PK-buffer, 10 µl SDS (10%) and 4.4 µl DTT (1 M) and incubated for 1 h at 60° C. 2 µl proteinase K (20 mg/ml) were added and incubation was continued for another 1 h. After addition of 30 µl NaCl solution (4.5 M) and incubation on ice for 10 min, specimens were centrifuged at 16.000 rcf for 20 min and the supernatant was transferred to a fresh reaction tube. 110 µl isopropanol were added and tubes were shaked carefully but thoroughly and centrifuged at 16.000 rcf for 20 min. The supernatant was discarded and 500 µl ethanol (70%) were added to wash the pellet. After storage over night at 4° C, tubes were centrifuged again at 16.000 rcf, 5 min, the ethanol was removed and the pellet air dried for 6 min. The pellet was then dissolved in 35 µl T-buffer and incubated for 1 h at 60° C. After vortexing, DNA was ready for further processing.

2.8.5 Screening of single-cell clones

To identify single-cell clones with mutations in the *OCT4* gene after transfection with CRISPR/Cas9, a PCR product from the mutation site was analyzed with Sanger sequencing. The PCR components were mixed on ice to a final volume of 25 µl in 0.2 ml reaction tubes. Previously isolated genomic DNA from single cell clones served as template and water was used as a non-template control. Details for master mix ingredients and PCR conditions are listed in Table 1 and Table 2.

Table 1: PCR components

Herculase II 5x reaction buffer	5.0 µl
dNTPs	2.5 µl
Forward Primer, 10 mM (OCT4 2f)	0.4 µl
Reverse primer, 10 mM (OCT4 2r)	0.4 µl
Herculase II Fusion DNA Polymerase	0.2 µl
Water	15.5 µl
Template	1.0 µl

Table 2: OCT4 PCR cycler protocol

Denaturation	4 min	95° C	
Denaturation	20 sec	95° C	x 35
Annealing	20 sec	56° C	
Elongation	40 sec	72° C	
Final elongation	10 min	72° C	
Termination	15 min	4° C	

For purification, PCR products were precipitated by adding 2.5 µl NaAc (3.5 M) and 60 µl ethanol (100%) and storage at -80° C for 30 min. After centrifugation for 30 min at 4° C and 16000 rcf, the pellet was washed in 100 µl ethanol (70%) and dissolved in 20 µl T-buffer. To verify presence and size of the PCR products, 2.5 µl bromophenolblue were added to 10 µl of precipitated PCR product and inserted to individual gel slots of a 1% agarose gel with 0.5 µg/ml ethidium bromide in a

chamber filled with TAE buffer. For determination of the fragment size, 6 µl of Gene Ruler™ 1 kb was added to an additional gel slot and an electrical field of 130 V was applied to start electrophoresis and after approximately 30 min, bands were visualized under UV-light. Positive PCR products were then used for the Sanger sequencing reaction, whose components and conditions are listed in Table 3 and Table 4.

Table 3: Sequencing reaction components

5x sequencing buffer	4 µl
BigDye	1 µl
Primer, 10 mM (OCT4 2f)	1 µl
Water	2 µl
Template	2 µl

Table 4: Sequencing reaction cycler protocol

Denaturation	1 min	95° C	
Denaturation	5 sec	95° C	x 40
Annealing	10 sec	52° C	
Elongation	4 min	60° C	
Termination	15 min	4° C	

To purify the products from the sequencing reaction, precipitation was essentially performed as described above. 2.5 µl EDTA (125 mM) and 30 µl ethanol (100%) were added and tubes were incubated on ice for 15 min. After centrifugation and washing with ethanol (70%), samples were dissolved in water and transferred to a 96-well sequencing plate. Analysis of the samples was carried out by the Genome Analysis Center at the Helmholtz Zentrum Munich. Sequences were analyzed with FinchTV Version 1.3.1 and the BioEdit Sequence Alignment Editor (HALL, 1999).

2.9 Somatic cell nuclear transfer

Somatic cell nuclear transfer experiments were conducted by PD Valeri Zakhartchenko as described in HIENDLEDER et al. (2004). Briefly, COCs were retrieved and matured as described in III.2.1. After 18-20 h of maturation, oocytes were denuded, treated with 5 µg/ml cytochalasin B and enucleated. Trypsinized somatic donor cells, cultured in starvation medium for 24 h, were placed into the perivitelline space and fused to the enucleated oocyte by applying a double electric pulse of 2.1 kV/cm for 10 µsec. 2 h after fusion, fused complexes were activated in ethanol (7%), followed by a 5 h culture in 10 µg/ml cycloheximide and 5 µg/ml cytochalasin B. After activation, cloned embryos were cultured as described in III.2.1.

2.10 Control embryos

To analyze the influence of ZP removal, PHA and overall handling on embryo development, day 5 embryos were exposed to SOF supplemented with 150 µg/ml PHA for 20 min in individual drops after removing the ZP, washed in SOF and transferred to a WoW culture dish. While removing the ZP of embryos for PHA exposure, a subset of embryos was kept outside the incubator in TL-HEPES-PVA as handling control for further culture in a WoW culture dish. To verify complete *OCT4* KO and to describe the *OCT4* KO phenotype, embryos derived from *WalterBF-Tg(PGK-EGFP)* fibroblasts served as controls in all experiments. Additionally, embryos reconstructed from the single cell clone *ETF1mut*^{2F11tm1} were produced to assess a possible effect of the off-target mutation in the *ETF1* gene (see IV.2.2).

2.11 Albertini fixation of embryos

For imaging, embryos were fixed in a microtubule stabilization buffer containing 2% paraformaldehyde (MESSINGER & ALBERTINI, 1991; LEIDENFROST et al., 2011). Fixation solution was prepared fresh and equlilibrated at 37° C every time. Embryos were washed in PBS supplemented with 0.1% PVA (PBS/PVA) and then transferred to the fixation solution and incubated at 37° C for 20 min. Fixed embryos were subsequently washed three times in PBS/PVA and stored in said medium at 4° C.

2.12 Imaging procedures

2.12.1 Imaging of chimeric embryos

After culture for 96 h, all chimeras were retrieved from the WoW culture dish and individual depressions within the WoW were checked for not-integrated aggregation partners. Only complete chimeras were considered blastocysts and evaluated for integration of eGFP positive donor blastomeres using an inverted epifluorescence microscope (Axiovert 200 M; Zeiss, Oberkochen, Germany) with the adequate filter set (excitation: 470/40, emission: 525/50). A subset of chimeras was stained for the TE-specific transcription factor CDX2 to differentially stain TE and ICM (MADEJA et al., 2013). Fixed blastocysts were incubated in a 1:200 dilution of rabbit anti-CDX2 polyclonal antibodies for 30 min at 37° C, washed three times in PBS/PVA and incubated in a 1:800 dilution of donkey anti-rabbit immunoglobulin G labeled with Alexa Fluor 555 for 30 min at 37° C. After washing again three times in PBS/PVA, blastocysts were placed on microscope slides in an antifade mounting medium with 40,6-diamidino-2-phenylindole (DAPI; VECTASHIELD) in a manner that conserves the three dimensional structure of the specimen (WUENSCH et al., 2007).

2.12.2 Immunofluorescent expression analysis

Before fixation of day 5 morulae and day 7-9 blastocysts, the ZP of non-hatched embryos was removed. Prior to staining, embryos were incubated for 1 h at room temperature in a blocking solution containing 0.5% Triton X-100 and 5% donkey serum. Simultaneous staining for either OCT4 and CDX2 or NANOG and GATA6 was achieved by incubation over night at 4° C in primary antibody solution and transfer to secondary antibody solution at 37° C for 1h after washing three times. For OCT4/CDX2 staining, dilution of goat anti-human OCT4 polyclonal antibodies and rabbit anti-human CDX2 polyclonal antibodies was 1:500 and 1:250, respectively. Secondary antibodies (donkey anti-rabbit Alexa Fluor 555 and donkey anti-goat Alexa Fluor 633) were both diluted 1:800. Staining of NANOG/GATA6 was performed with rabbit anti-human NANOG at 1:500 and goat anti-human GATA6 at 1:250 with secondary antibodies at 1:500 (donkey anti-rabbit Alexa Fluor 555) and 1:400 (donkey anti-goat Alexa Fluor 633). After washing, embryos were embedded

as described above. Specific binding of secondary antibodies was ensured by omitting the first antibody and possible cross-reactivity between primary and secondary antibodies was excluded by labeling one primary antibody with the secondary antibody specific to the other primary antibody in a simultaneous staining and vice versa. To control if secondary antibodies are binding incorrectly to each other, samples were incubated without the primary antibodies.

2.12.3 Confocal microscopy

Stacks of optical sections were recorded using an LSM710 Axio Observer confocal laser scanning microscope (CLSM; Zeiss) with an interval of 2.5 µm using a x25 water immersion objective (LD LCI Plan-Apochromat 25x/0.8 Imm Korr DIC M27) and a pinhole of 32 µm. The settings for imaging of chimeras and expression analysis are presented in Table 5.

Table 5: Settings for confocal laser scanning microscopy of embryos and chimeras. Wavelength of excitation/emission, laser line and filter in nm.

	Target	Dye/ fluorophore	Excitation/ Emission	Track	Laser line	Filter
Expression analysis	DNA	DAPI	358/461	Track 1	405	410 - 562
	OCT4	Alexa 633	632/648	Track 1	633	638 - 747
	CDX2	Alexa 555	553/568	Track 2	561	582 - 631
	NANOG	Alexa 555	632/648	Track 2	561	562 - 611
	GATA6	Alexa 633	553/568	Track 1	633	638 - 747
Chimeras	CDX2	Alexa 555	553/568	Track 1	561	566 - 697
	eGFP cells	eGFP	488/509	Track 2	488	494 - 552

2.12.4 Image analysis

Images were analyzed with icy bioimage analysis software (DE CHAUMONT et al., 2012) using the manual counting plug-in, in which every slide of an image stack was analyzed individually to avoid double cell counts. The number of total cells was assessed by counting all the nuclei stained with DAPI, the number of TE, HB and EPI cells was determined by counting all the nuclei co-stained with DAPI and CDX2, GATA6 and NANOG, respectively. The number of cells in the ICM was calculated by subtracting the number of TE cells from the total cell number. Figures were produced with Fiji software (SCHINDELIN et al., 2012).

2.13 Statistical analysis

All data were analyzed with GraphPad Prism 5.02 using the two-tailed unpaired t test or the 1way ANOVA with Tukey‘s multiple comparison test for comparison of cell numbers and blastocyst rates. Fisher’s exact test was used for the development of wild-type chimeras and control embryos. Level of significance was set to $P<0.05$ and data are presented as mean ± standard deviation (SD).

IV. Results

1. Chimeras with wild-type host embryos

Results in this section have been published in SIMMET et al. (2015a), including Figures 7-9 and Tables 6-8.

1.1 Host and donor embryo development

1621 presumptive zygotes were produced for host embryos. 1370 (84.5%) did not complete their first cleavage until 27 h after IVF. Of these zygotes, 928 (52.7%) cleaved and 489 (35.7%) developed to day 4 morulae. A subset of host embryos (n=601) was cultured until day 7, of which 155 (25.8%) developed to blastocysts while in control embryos (n=506), that were not sorted according to timing of first cleavage, 210 (37.8%) developed to blastocysts (unpaired two-tailed t-test, $P<0.05$). For donor embryo production, 1744 presumptive zygotes were produced and 360 (20.7%) developed to day 5 morulae. 169 morulae were analyzed for eGFP expression using fluorescent microscopy, of which 76 (45%) were eGFP positive. A subset of 150 zygotes was cultured until day 7, of which 23 (15.3%) developed to blastocysts with 17 (73.9%) showing eGFP fluorescence.

1.2 Chimera development and donor blastomere integration

Development of chimeras aggregated with PHA or by the sandwich technique and the respective integration of eGFP positive donor blastomeres to ICM, TE or both lineages is shown in Table 6 and Figure 7. Developmental kinetics of chimeras, as recorded with the embryo monitoring system, are shown in Figure 8.

Table 6: Development of chimeras and donor blastomere integration using the different aggregation techniques. Different superscripts within a row indicate significant differences (Fisher's exact test, P<0.05). Adapted from SIMMET et al. (2015a).

	PHA	Sandwich
N° chimera	99	46
Blastocysts	85 (85.9%[a])	25 (54.3%[b])
GFP ICM	34 (40%[a])	4 (16%[b])
GFP ICM + TE	17 (20%[a])	11 (44%[b])
No GFP	33 (38.8%[a])	10 (40%[a])
GFP TE	1 (1.2%)	0

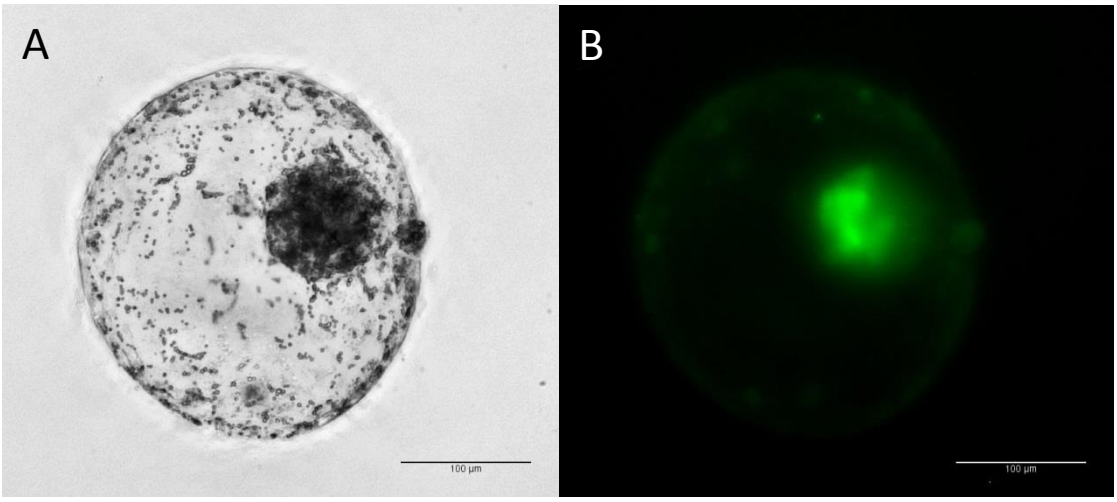

Figure 7: Chimera produced with PHA and donor embryo integration to the ICM. A: bright field with extended focus. B: eGFP positive donor cells in the ICM. Adapted from SIMMET et al. (2015a).

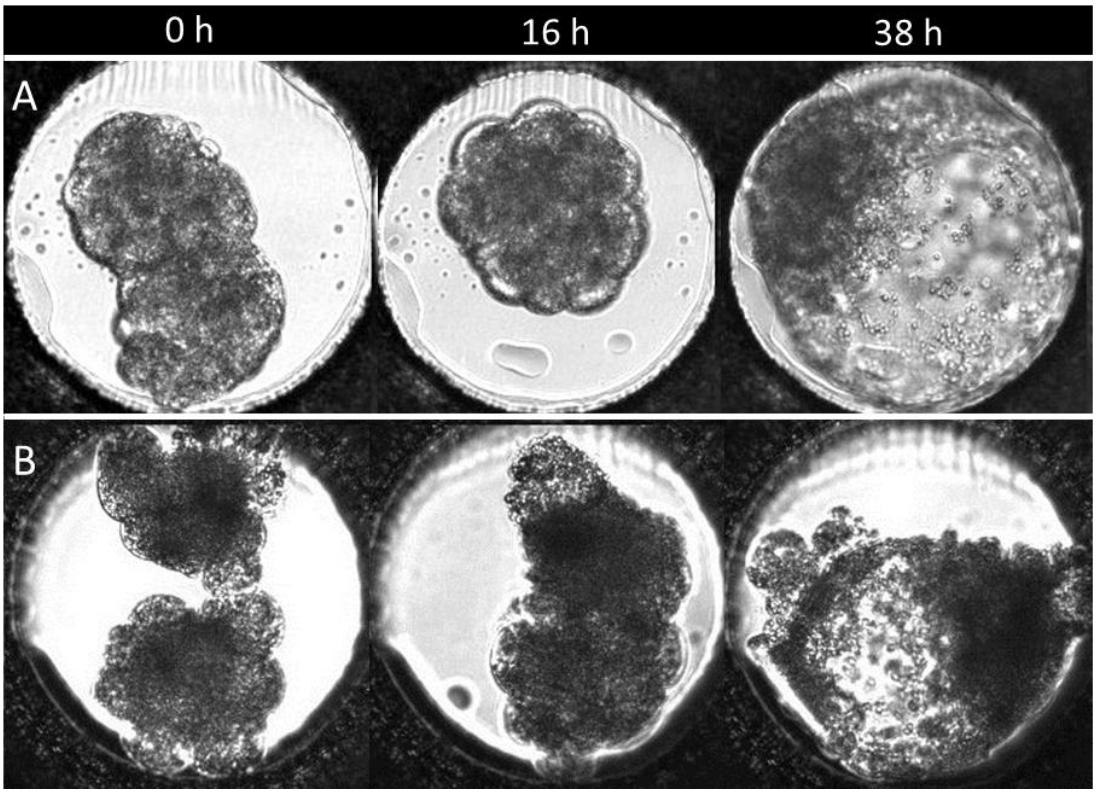

Figure 8: Development of chimeras aggregated with PHA (A) and by the sandwich technique (B) at 0 h, 16 h and 38 h after aggregation. Adapted from SIMMET et al. (2015a).

1.3 Cell numbers

Cell numbers of chimeras produced with PHA, embryos exposed to PHA and handling control embryos are shown in Table 7. Development from day 5 morula to day 9 blastocyst was 43/54 (79.6%) for embryos exposed to PHA and 23/32 (71.9%) for handling control embryos (P>0.05).

Table 7:Mean ± SD of number of total cells, number of ICM cells, number of TE cells and ratio of ICM/total cells of chimeras (n=17), embryos exposed to PHA (n=30) and handling control embryos (n=19). Different superscripts within a row indicate significant differences (unpaired two-tailed t-test, P<0.05). Adapted from SIMMET et al. (2015a).

	Chimera	PHA	Handling Control
Total cell number	207.8 ± 68.3[a]	159.6 ± 42.2[b]	176.9 ± 53.3[b]
ICM	56.5 ± 22[a]	37.7 ± 14.2[b]	38.7 ± 12.4[b]
TE	151.2 ± 58[a]	121.9 ± 37.4[b]	138.3 ± 53[a, b]
ICM/Total	27.9% ± 8.8	23.1% ± 7.9	24% ± 8

1.4 CLSM analysis of chimeras with wild-type hosts

Of 17 analyzed chimeras by CLSM, 8 showed no eGFP expression and 9 chimeras showed donor blastomere integration to the ICM, the TE or both lineages. Three blastocysts showed integration of eGFP positive blastomeres to the ICM with 16, 14 and 5 blastomeres, respectively. Each 10, 4 and 2 eGFP blastomeres colonized the TE and integration to both cell lineages occurred in three blastocysts with 8 and 1, 5 and 1, and 2 and 2 blastomeres integrated to the ICM and TE, respectively. Further cell number data on chimeras are presented in Table 8 and representative images of a chimera are shown in Figure 9.

Table 8: Cell counts of chimeric blastocysts including number of eGFP positive cells according to allocation of eGFP positive blastomeres (mean ± SD). Adapted from SIMMET et al. (2015a).

	Total cell number	TE	ICM	eGFP ICM	eGFP TE
Chimeras with eGFP in ICM (n=3)	251.3 ± 39.6	172.3 ± 39.3	79 ± 23.3	11.67 ± 5.9	-
Chimeras with eGFP in ICM and TE (n=3)	154.3 ± 53.7	103.3 ± 34.6	51 ± 32.1	5 ± 3	1.3 ± 0.6
Chimeras with eGFP in TE (n=3)	142.7 ± 45.4	111 ± 45.4	31.7 ± 9.1	-	5.3 ± 4.2
Chimeras with no eGFP (n=8)	235.9 ± 63.7	176.4 ± 61	59.5 ± 11.2	-	-

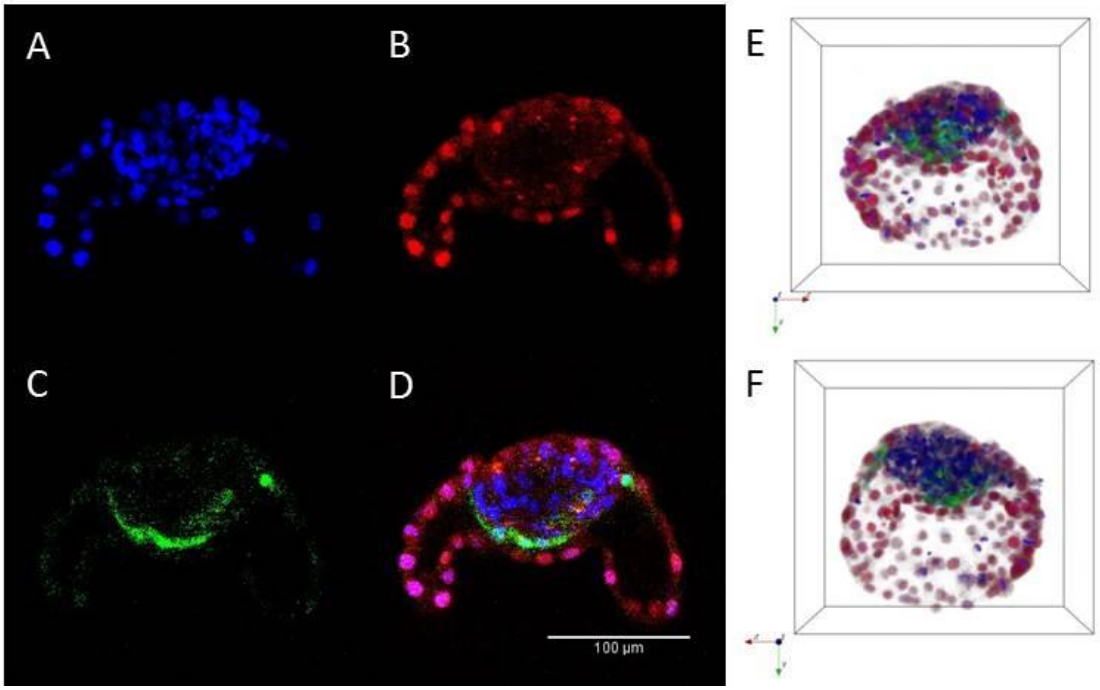

Figure 9: Single slices and 3D projection of CLSM image of a chimera with eGFP donor blastomere integration to the ICM. A: all nuclei stained with DAPI. B: TE cells stained with anti-CDX2 antibody. C: eGFP positive blastomeres. D: merged image of A, B and C. E, F: two images from different angles (0° and 180°). Adapted from SIMMET et al. (2015a).

2. *OCT4* knockout embryos

2.1 CRISPR/Cas9 targeting efficiency

After seeding the transfected cells on ten 96-well half area culture plates, 156 single cell clones were identified, propagated and screened for mutations, resulting in a total of 4 (2.6%) single cell clones with mutations. One single cell clone (*WalterBF-Tg(PGK-EGFP)POU5F1*^{1AH1tm1}), which was used for further experiments, carried a biallelic deletion of a single nucleotide that leads to a frameshift mutation (Figure 10). The biallelic mutation was confirmed with the continuous chromatogram from Sanger sequencing downstream of the deletion (Figure 10) and with a conserved SNP 200 bp downstream from the PAM (Figure 11), sequenced with the OCT4 11f primer.

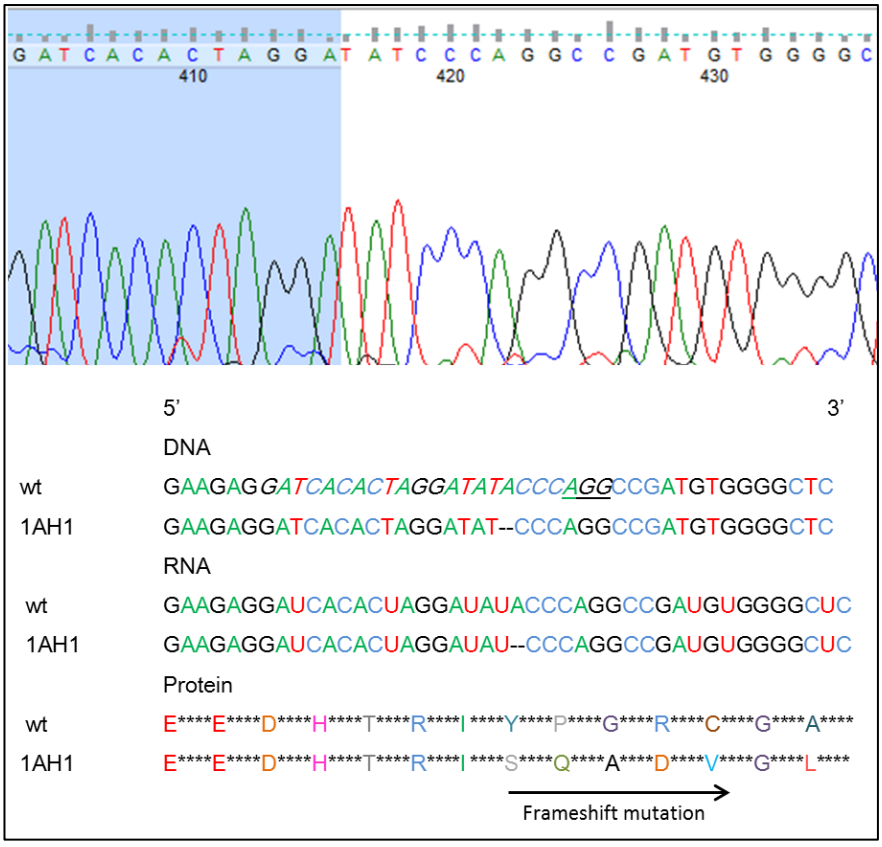

Figure 10: Chromatogram and mutation of WalterBF-Tg(PGK-EGFP)POU5F1^{1AH1tm1} *on DNA, RNA and protein level; "wt" represents the reference genome (NCBI gene ID: 282316) with sgRNA in italics and the PAM underlined.*

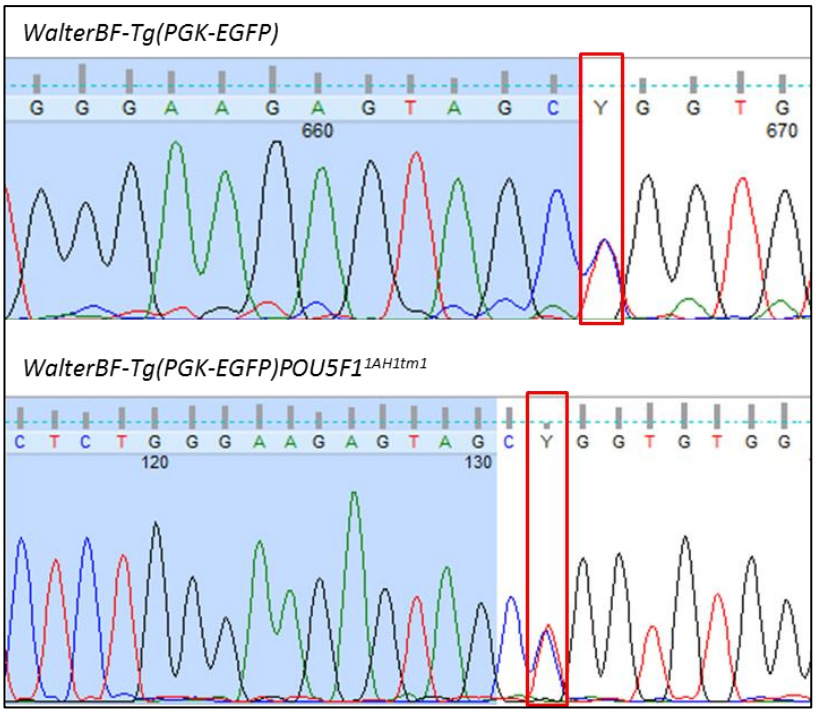

Figure 11: Chromatogram of conserved SNP 200 bp downstream from mutation site in non-transfected cells (WalterBF-Tg(PKG-EGFP)) and mutated single cell clone (WalterBF-Tg(PKG-EGFP)POU5F1^{1AH1tm1}).

2.2 CRISPR/Cas9 off target effects

Because *OCT4* is silenced in somatic cells, a low targeting efficiency due to a low accessibility of the gene was assumed when designing the sgRNA. Therefore, from the sgRNAs generated by chopchop software, the most promising sgRNA regarding specificity and efficiency scores was used (boOCT4 sgRNA, see III.1.5). Also, to cover all OCT4 isoforms, exon 2 was selected as sgRNA binding site, as this exon is included to all known splicing variants of the human OCT4 protein (WANG & DAI, 2010). A pitfall in designing the sgRNA for the bovine *OCT4* locus, is the presence of an *OCT4* pseudogene, where the *OCT4* transcript, including exon 1-4 and the first 27 bp of exon 5, is integrated to the first intron of the eukaryotic translation termination factor 1 gene (*ETF1*) on chromosome 7 (SCHIFFMACHER & KEEFER, 2013). The boOCT4 sgRNA was analyzed for off-target effects with the web application e-crisp (HEIGWER et al., 2014), which also offers the bovine reference genome. The same specificity and efficiency scores as for the *OCT4* target were found within the *ETF1* gene, but it was not possible to design a different sgRNA that meets the above mentioned requirements (high efficiency and coverage of all

splicing variants) without targeting the *OCT4* pseudogene. Therefore, the off target site of 22 single cell clones was analyzed for mutations to examine the degree of the off target effects. The locus was amplified with primers ETF1 2f and ETF1 2r and then sequenced with the primers ETF1 3f and ETF1 2r; 8 (36%) clones carried a mutation, including *WalterBF-Tg(PKG-EGFP)POU5F1*^{1AH1tm1}. Its monoallelic mutation of a single nucleotide is shown in Figure 12, where the chromatograms of the forward and reverse sequences both break up at the same position, due to a deleted nucleotide on one allele.

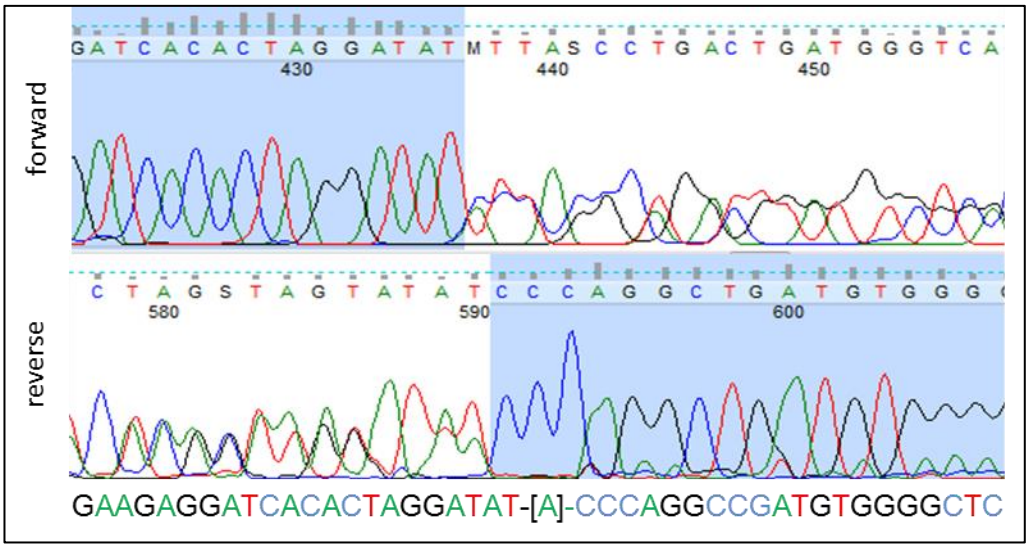

Figure 12: Monoallelic deletion of a single nucleotide (in brackets) on off target site in single cell clone WalterBF-Tg(PKG-EGFP)POU5F1^{1AH1tm1}.

We identified one single cell clone (*ETF1mut*^{2F11tm1}) that carries the exact same mutation as *WalterBF-Tg(PKG-EGFP)POU5F1*^{1AH1tm1} in the *ETF1* off target gene but no mutation in the *OCT4* gene. Embryos reconstructed from these cells served as additional controls to identify possible effects of the mutation in *ETF1* on developmental rates.

2.3 Somatic cell nuclear transfer

To analyze the phenotype of embryos derived from the single cell clone *WalterBF-Tg(PGK-EGFP)POU5F1*^{1AH1tm1} (*OCT4* KO), and thereby the effect of an *OCT4* KO in bovine preimplantation embryos, embryos were reconstructed with SCNT. Embryos derived from the non-transfected cell line *WalterBF-Tg(PGK-EGFP)* served as controls (NT CTRL). Morphology of the embryos at day 7 and day 9,

including eGFP expression (recorded as described in III.2.12.1), is shown in Figure 13. By day 7, *OCT4* KO and NT CTRL embryos showed normal blastocyst morphology with a discernable ICM and TE, also blastocysts began to expand by day 7 as evidenced by a thinner ZP. At day 9, blastocysts of both groups were able to hatch from the previously opened ZP (assisted hatching) and NT CTRL blastocysts evidently exceeded *OCT4* KO blastocysts in size. Both groups expressed eGFP until day 9.

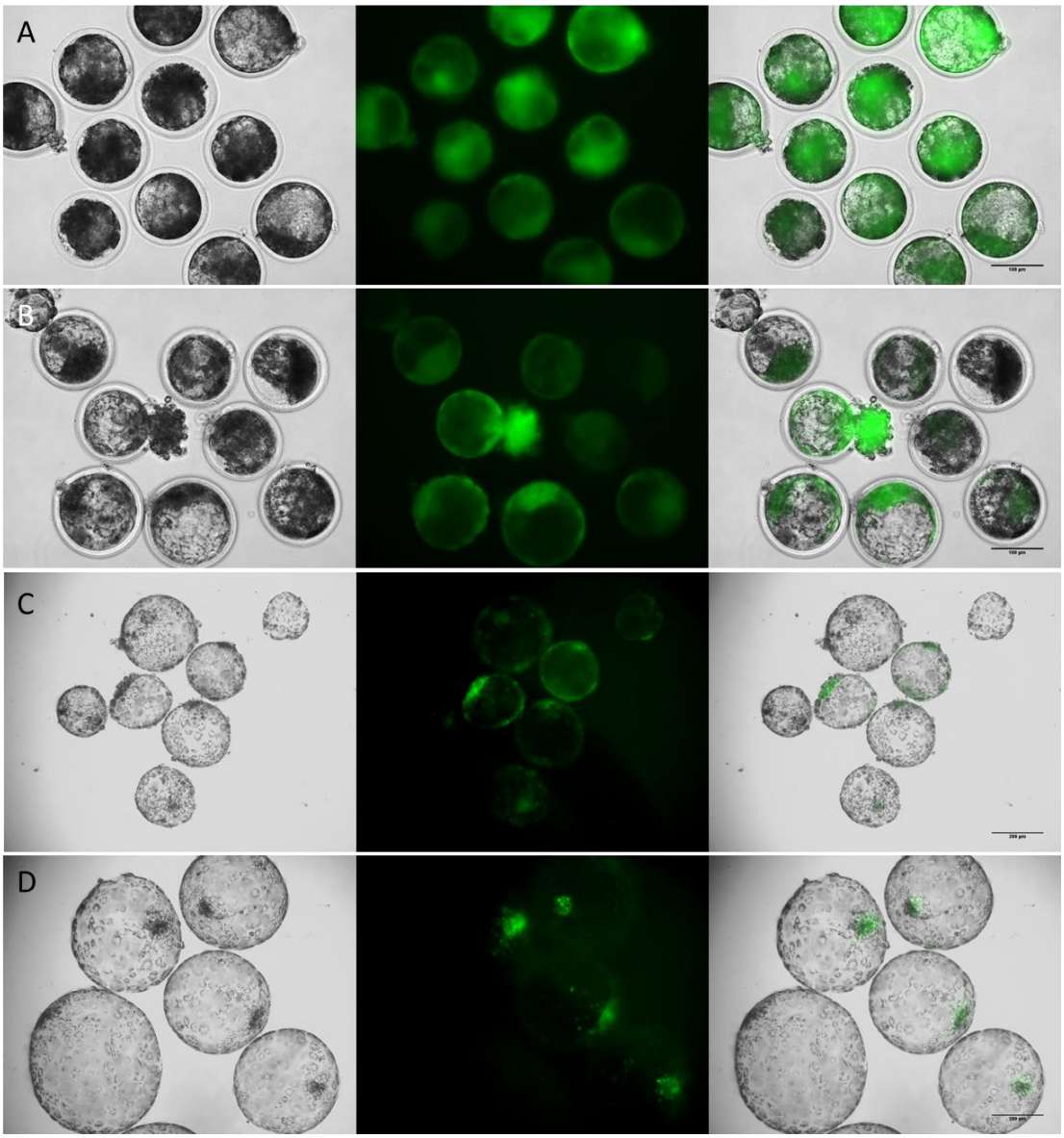

Figure 13: Brightfield images with extended focus, eGFP expression and the merge of OCT4 KO (A) and NT CTRL (B) day 7 blastocysts and OCT4 KO (C) and NT CTRL (D) day 9 hatched blastocysts. Scale bars represent 100 µm.

Developmental rates of *OCT4* KO and NT CTRL embryos are presented in Table 9. There was no significant difference in cleavage rate or development to morula stage between *OCT4* KO and NT CTRL; blastocyst rate by day 7 was strongly decreased in *OCT4* KO embryos because of a lower morula to blastocyst transition rate.

Table 9: Development of cloned embryos to day 7 blastocysts. Rates are calculated based on the number of successful fusions and presented as mean [%] ± SD; [n] represents the number of experiments. Different superscripts within a row indicate significant differences (P<0.05, unpaired, two-tailed t-test).

	WalterBF-Tg(PGK-EGFP)OCT4ko^{1AH1tm1} n=21	*WalterBF-Tg(PGK-EGFP)* n=18
N° constructs	765	474
Fused (fusion rate)	741 (96.3 ± 4^{a})	439 (91.8 ± 5.7^{b})
Cleaved (cleavage rate)	516 (69.5 ± 13.1^{a})	266 (64.4 ± 13.1^{a})
Day 5 morula (morula rate)	252 (34.7 ± 18.7^{a})	153 (36.1 ± 11.6^{a})
Day 7 blastocyst (blastocyst rate)	125 (16.78 ± 10.21^{a})	135 (32.07 ± 10.84^{b})
Blastocysts/morula	45.78 ± 24.54^{a}	89.27 ± 11.39^{b}

213 fused constructs were produced with the single cell clone *ETF1mut*^{2F11tm1} (see IV.2.2) in three experiments. There was no significant difference (P>0.05, 1-way ANOVA with Tukey's Multiple Comparison Test) to the development of NT CTRL or *OCT4* KO embryos with a blastocyst rate of 22.6 ± 8.8% (mean ± SD).

2.4 Immunofluorescence analysis

2.4.1 OCT4 and CDX2

To confirm the absence of OCT4 protein in *OCT4* KO embryos and to differentially stain ICM and TE in blastocysts, day 5 morulae and day 7 blastocysts from *OCT4* KO, NT CTRL and from *in vitro* produced embryos (IVP CTRL) were stained against OCT4 and CDX2 simultaneously. Only day 5 morulae that exceeded a total cell count of ≥ 32 cells were included to the analysis. While NT CTRL and IVP CTRL morulae expressed OCT4 in all cells, *OCT4* KO morulae showed expression in only 67.8% ± 11.1 (mean ± SD, n=6) of cells and overall intensity was decreased. In none of the embryos, CDX2 was expressed in the nuclei but detected in the cytoplasm (Figure 14).

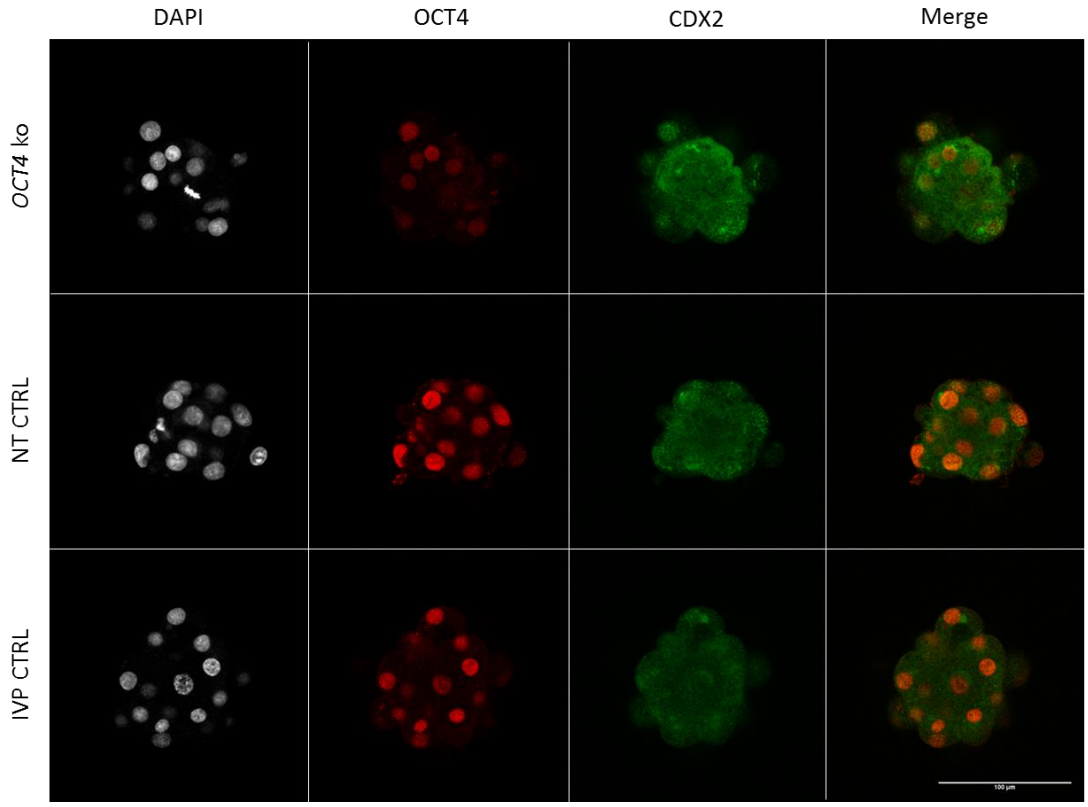

Figure 14: Single slices of confocal images of day 5 morulae stained against OCT4 and CDX2.

In day 7 blastocysts, OCT4 was no longer detectable in *OCT4* KO embryos, while control embryos ubiquitously expressed OCT4. In all embryos, CDX2 was expressed in the nuclei and restricted to TE cells (Figure 15).

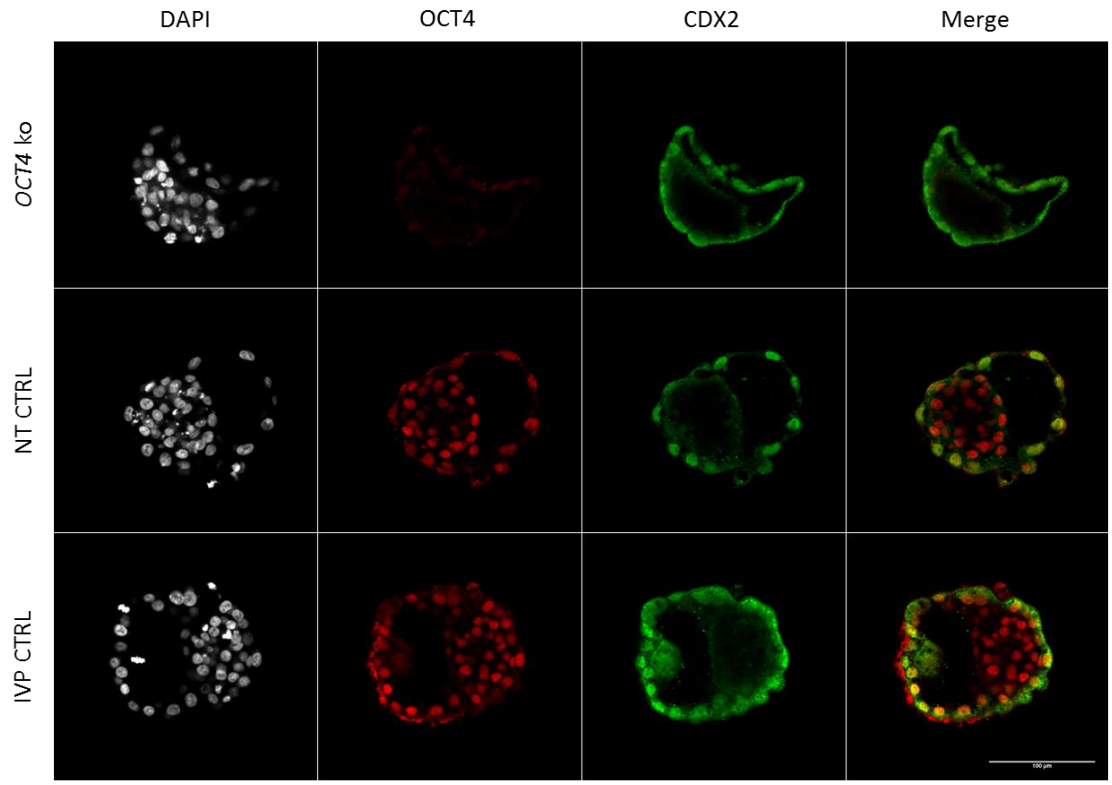

Figure 15: Single slices of confocal images of day 7 blastocysts stained against OCT4 and CDX2.

The number of total cells and the percentage of OCT4 and CDX2 positive cells for day 7 blastocysts from SCNT (*OCT4* KO and NT CTRL) and from embryos derived from *in vitro* fertilization (IVP CTRL) are shown in Table 10.

Table 10: Total cell number and percentage of OCT4 and CDX2 positive cells for OCT4 KO, NT CTRL and IVP CTRL day 7 blastocysts. [n] represents number of analyzed blastocysts per group. Different superscripts within a row indicate significant differences (P<0.05, 1way ANOVA with Tukey's multiple comparison test).

	OCT4 KO	NT CTRL	IVP CTRL
	n=24	n=20	n=40
Total cell number	89.6 ± 27.5[a]	96.3 ± 38[a]	125.8 ± 36.5[b]
[%] OCT4 positive cells	0[a]	78.8 ± 10.5[b]	77.2 ± 16.4[b]
[%] CDX2 positive cells	56.8 ± 11.5	62.5 ± 9.6	59.3 ± 9.2

2.4.2 NANOG and GATA6

To investigate the role of OCT4 during the second lineage differentiation, day 5 morulae, day 7 blastocysts and day 9 hatched blastocysts were analyzed for expression of the HB and EPI specific markers GATA6 and NANOG, respectively. At day 5, all embryos co-expressed both markers and *OCT4* KO embryos showed the same expression pattern as NT CTRL and IVP CTRL embryos (Figure 16), although the percentage of GATA6 positive cells was significantly decreased. Detailed data for total cell numbers and percentage of GATA6 and NANOG positive cells in day 5 morulae is provided in Table 11.

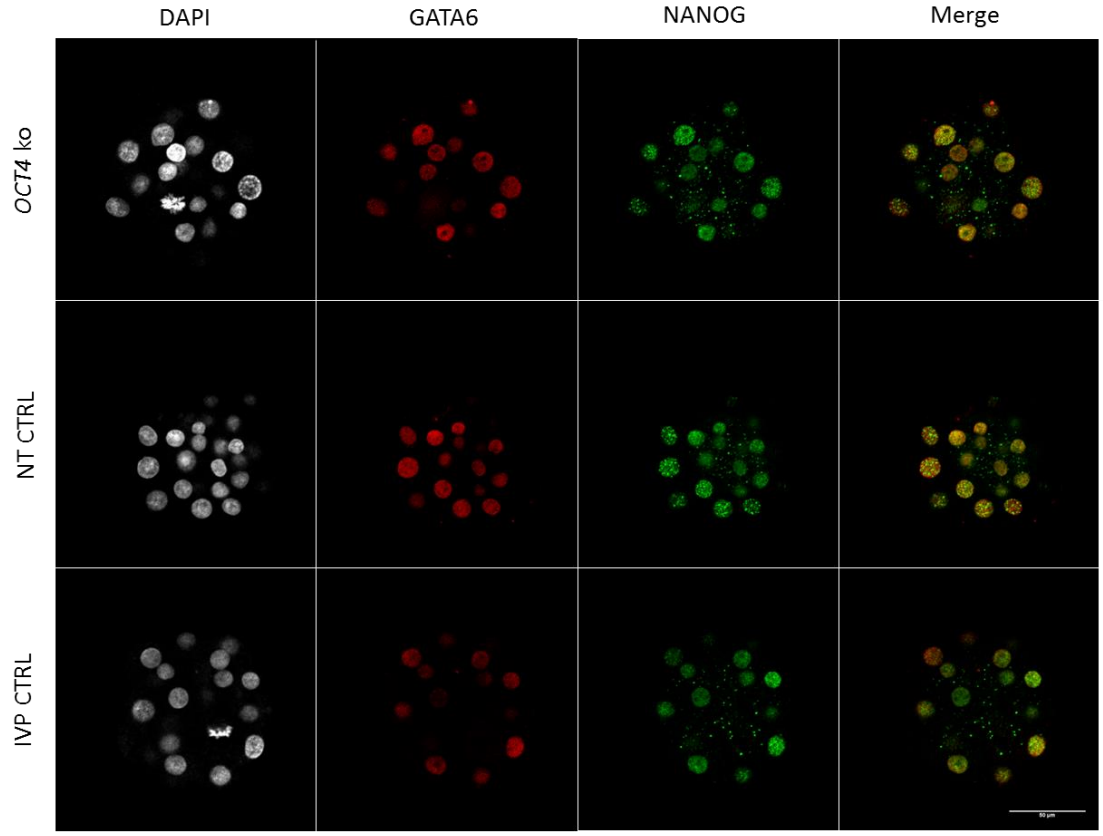

Figure 16: Single slices of confocal images of day 5 morulae stained against GATA6 and NANOG.

Table 11: Total cell number and percentage of GATA6 and NANOG positive cells for OCT4 KO, NT CTRL and IVP CTRL day 5 morulae. [n] represents number of analyzed morulae per group. Different superscripts within a row indicate significant differences (P<0.05, 1way ANOVA with Tukey's multiple comparison test).

	OCT4 KO	NT CTRL	IVP CTRL
	n=9	n=14	n=7
Total cell number	55 ± 13.3	65.9 ± 15.7	56.1 ± 12
[%] GATA6 positive cells	60.4 ± 13.9[a]	92.7 ± 7.7[b]	89.5 ± 5.5[b]
[%] NANOG positive cells	80.5 ± 9.2[a]	92.9 ± 7[b]	84.7 ± 10.3[a,b]

In day 7 blastocysts, NT CTRL (n=13) and IVP CTRL (n=6) embryos already showed the typical salt and pepper distribution of NANOG and GATA6 positive cells, but expression was not mutually exclusive in all cells. When the factors were co-expressed, fluorescent intensity of both was decreased, compared to their exclusive expression. Also expression was not restricted to the ICM, as cells from the TE also still stained positive for both markers (Figure 17). In SCNT CTRL day 7 blastocysts, 7.1 ± 2.9% and 9.8 ± 4% of cells stained exclusively positive for NANOG and GATA6, respectively (n=13, mean ± SD, unpaired two-tailed t-test, P>0.05). *OCT4* KO embryos (n=8) lost all NANOG expression at day 7 blastocyst stage and only stained positive for GATA6 in a similar pattern as NT CTRL blastocysts with a few cells of higher intensity (Figure 17).

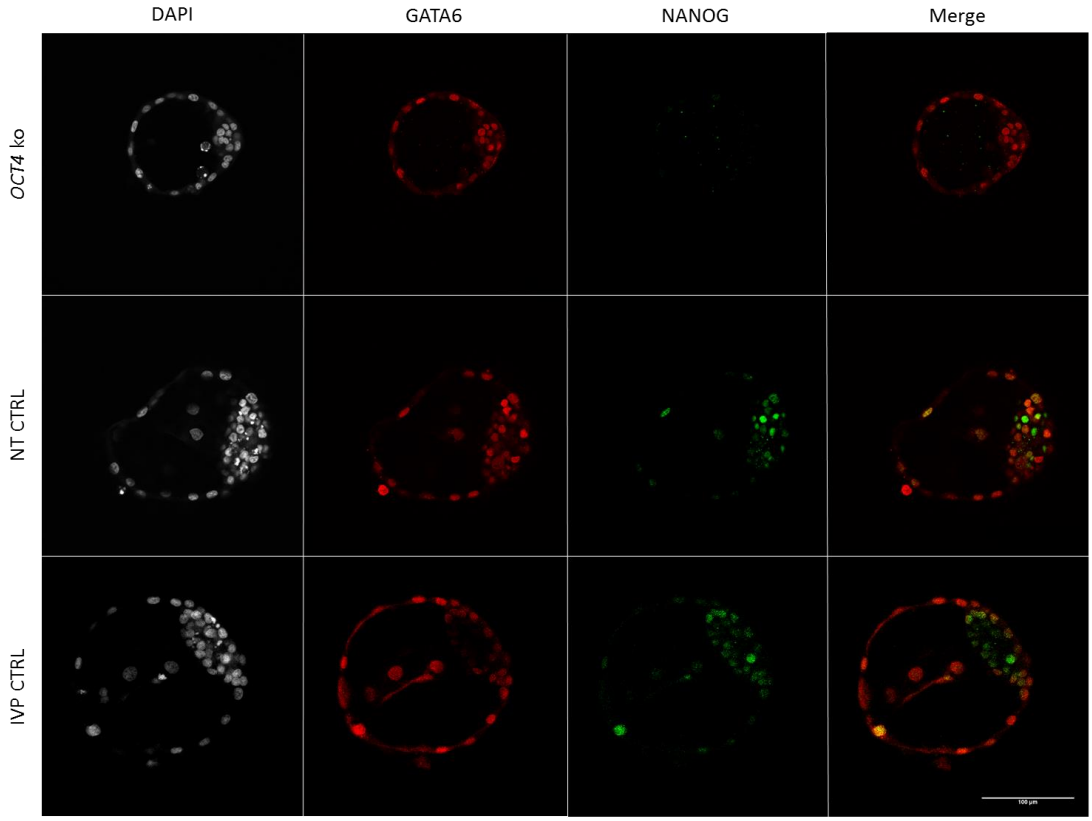

Figure 17: Single slices of confocal images of day 7 blastocysts stained against GATA6 and NANOG.

Expression of NANOG and GATA6 was mostly limited to cells of the ICM and mutually exclusive in NT CTRL (n=7) and IVP CTRL (n=3) day 9 hatched blastocysts (Figure 18). *OCT4* KO blastocysts (n=6) showed no expression of NANOG or GATA6, also there were no packed cells as indicative for an ICM. The total cell number of *OCT4* KO embryos (n=6) was strongly decreased when compared to NT CTRL (n=7) by day 9 (139.2 ± 33.5 vs. 319.7 ± 70.51, mean ± SD, unpaired two-tailed t-test, $P<0.05$)

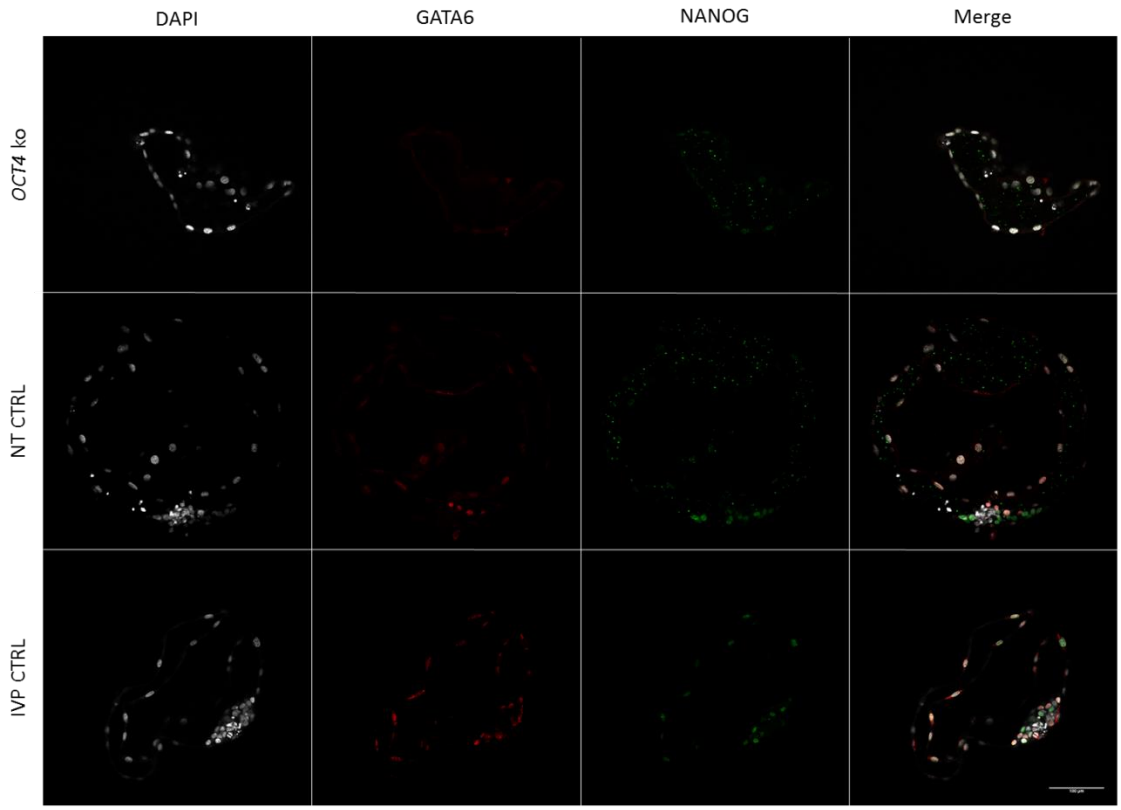

Figure 18: Single slices of confocal images of day 9 hatched blastocysts stained against GATA6 and NANOG.

After *in vitro* culture for 9 days, cells from the ICM predominantly contained degenerated cell nuclei in all embryos, so the majority of cells in the ICM could not be examined for expression of EPI or HB specific markers (Figure 19). This made further analysis of events during the second lineage differentiation in *in vitro* cultured day 9 blastocysts futile.

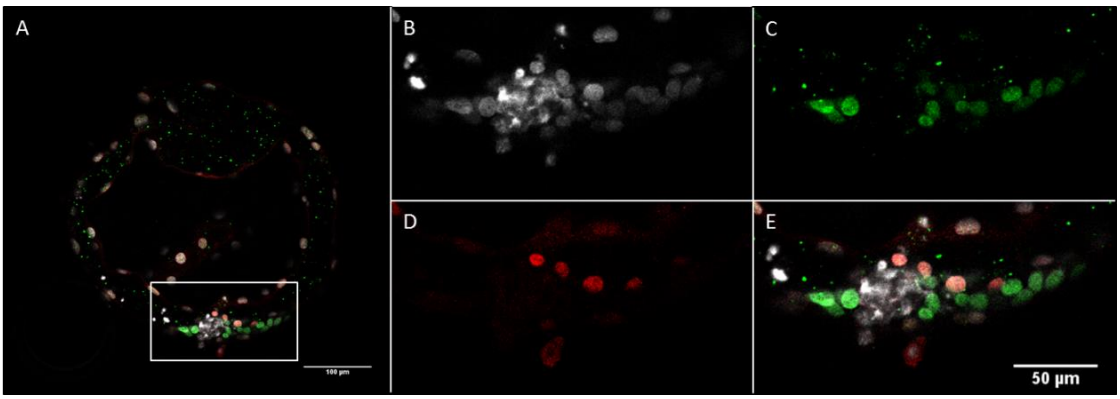

Figure 19: Day 9 hatched NT CTRL blastocyst cultured in vitro. A: single slice of a confocal image with NANOG (green), GATA6 (red) and nuclei counterstained with DAPI (grey). Rectangle in A marks enlarged ICM, shown in B (DAPI), C (NANOG), D (GATA6) and E (merge of B,C and D).

3. Chimeras with *OCT4* KO host embryos

Chimeras with *OCT4* KO host embryos from SCNT and wild-type donor cells from IVP embryos were produced like chimeras with wild-type hosts, except asynchronic aggregation, which was omitted to solely study the effect of *OCT4* KO in hosts on donor blastomere integration in the chimera (see III.2.5). In four experiments using day 4 morulae as hosts and donors, 32 aggregates were cultured of which 24 (74 ± 28.1%, mean ± SD) developed to blastocysts. Developmental kinetics of chimeras with *OCT4* KO hosts did not differ from development of wild-type embryos aggregated with PHA, showing the same tight compaction of the aggregation partners to one morula before developing the blastocyst cavity (Figure 20).

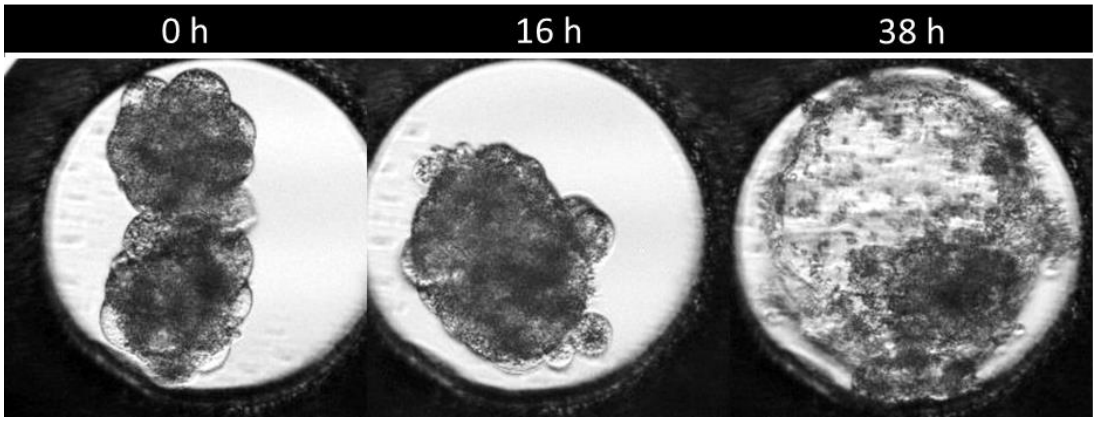

Figure 20: Development of chimera with OCT4 *KO embryos as hosts at 0 h, 16 h and 38 h after aggregation.*

At 96 h after aggregation, expansion of the blastocyst was not as marked as in wild-type chimeras and when washing the developed blastocysts before fixation, they lost a substantial amount of loosely attached cells, which was not observed with chimeras from wild-type donor hosts. Brightfield and eGFP fluorescence images from a developed chimeric blastocyst are shown in Figure 21.

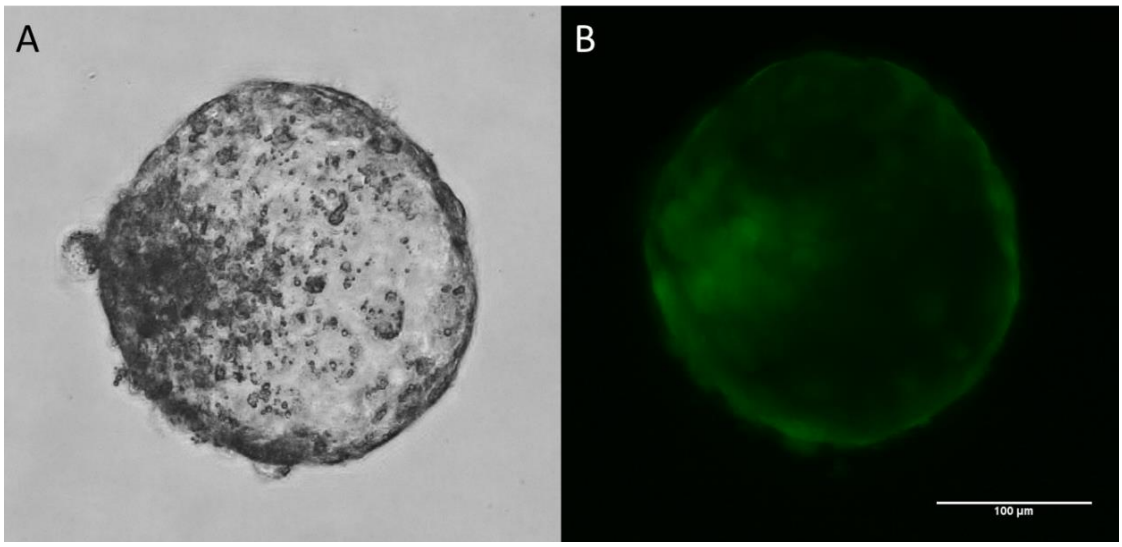

Figure 21: Chimera produced with two OCT4 *KO host embryos and four wild-type blastomeres at day 4. A: bright field with extended focus. B: eGFP expression with extended focus.*

13 chimeric blastocysts stained against CDX2 and OCT4 were analyzed with CLSM and 7 showed integration of donor blastomeres, as evidenced by the presence of OCT4 and the absence of eGFP in cells derived from the donor embryo. Co-staining with CDX2 allowed determination of lineage allocation of the aggregation partners (Figure 22). Donor cells colonized the ICM in 2 chimeric blastocysts with 8 and 15 cells, making up 27.6% and 38.5% of the ICM, respectively. 2 chimeras with OCT4 positive cells in the TE had a total cell number underneath the average of *OCT4* KO day 7 blastocysts (see Table 10) with 69 and 67 cells, respectively. Further data on total cell number and percentage of OCT4 and CDX2 positive cells is presented in Table 12.

Table 12: Total cell number and percentage of OCT4 and CDX2 positive cells for chimeras with OCT4 *KO host embryos. [n] represents number of analyzed blastocysts per group.*

	Chimeras without OCT4 (n=6)	Chimeras with OCT4 in TE (n=5)	Chimeras with OCT4 in ICM and TE (n=2)
Total cell number	155.8 ± 37.1	123.3 ± 54.9	158 ± 22.6
[%] OCT4 positive cells	-	36.1 ± 19.6	21.9 ± 5.8
[%] CDX2 positive cells	68.9 ± 12.3	72.2 ± 10.9	78.6 ± 1.4

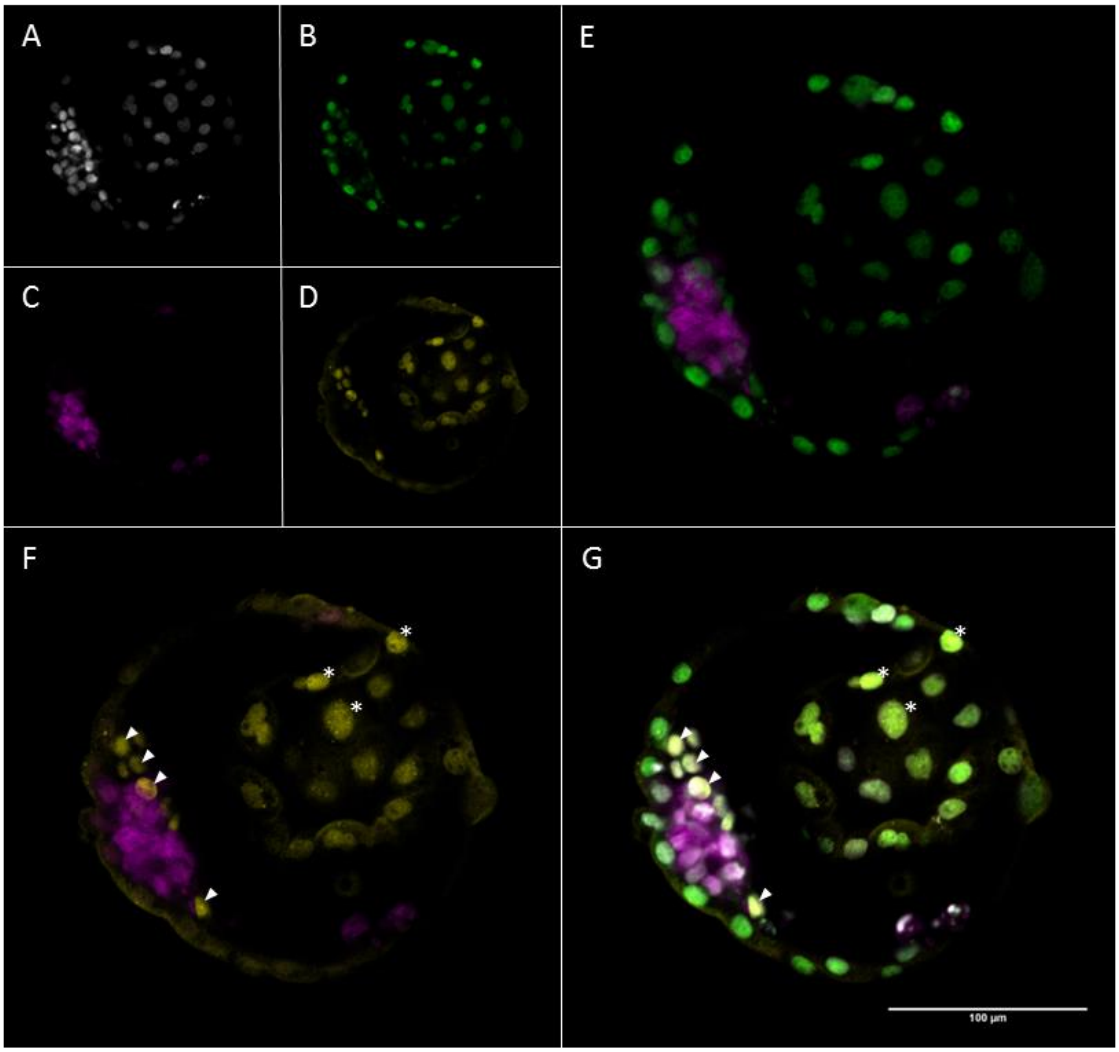

Figure 22: Single slices of confocal images of chimera produced with two OCT4 *KO host embryos and four wild-type blastomeres stained against OCT4 and CDX2. A: all nuclei stained with DAPI. B: TE cells stained with anti-CDX2 antibody. C: eGFP positive blastomeres from* OCT4 *KO hosts. D: OCT4 positive cells from donor. E: merge of B and C. F: merge of C and D. G: merge of A, B, C and D. Arrowheads and asterisks in F and G exemplarily show donor cells in the ICM and TE, respectively.*

V. Discussion

With the upcoming of genomic estimated breeding values (GEBV), the commercial value for positively selected embryos has increased dramatically. Therefore, a reliable embryo multiplication technique that is technically undemanding and highly efficient is sought. Multiplication of genotypes using chimeric complementation is a promising approach, because the techniques involved are relatively simple and resulting offspring does not suffer from artefacts associated to the method. Still, a major hurdle is to exclude host-embryo cells from the pluripotent lineage, so the fetus proper only develops from the desired genotype. Previous approaches using tetraploid complementation, as performed in the mouse, failed with bovine embryos, probably because electrofusion at the two-cell stage does not result in uniformly tetraploid embryos. In this thesis, new strategies for embryo multiplication via chimera complementation were examined, including the use of genetically modified host embryos that carry a KO of the pluripotency gene *OCT4*. In addition, this is to my knowledge the first report on the effects of an *OCT4* KO in the bovine preimplantation embryo.

Donor cells aggregated with wild-type host embryos fail to establish exclusively in the ICM of chimeras

In chimeras aggregated from wild-type host embryos and transgenic donor blastomeres, eGFP expression enabled quantitative and spatial analysis of donor integration to the chimera, i.e. the number of donor-derived cells and their respective integration to ICM or TE. The eGFP transgenic donor embryos were produced by IVF using semen from an eGFP transgenic founder bull (“Jojo”), which was produced by lentiviral trangenesis and carries seven proviral integrants that segregate independently (HOFMANN et al., 2004; REICHENBACH et al., 2010). The rate of eGFP positive F1 embryos depends on the transmitted integrants and on possible epigenetic silencing of the reporter construct (HOFMANN et al., 2006), which in this study resulted in 45% and 73.9% eGFP positive day 5 morulae and day 7 blastocysts, respectively. Expression of eGFP additionally remains stable until day 15 in embryos and day 45 in fetuses (REICHENBACH et al., 2010), which would allow the use of

this system in experiments, where later developmental stages and allocation of the aggregation partners to different tissues or cell lineages, e.g. the primordial germ cell line, is of interest.

To promote integration of the donor blastomeres to the ICM and to bias cells from the host embryos towards differentiation to extraembryonic tissues, host embryos that did not complete their first cleavage until 27 h after IVF were selected. These embryos contain more blastomeres with chromosomal aberrations (SUGIMURA et al., 2012), which are preferentially allocated in the TE. This is evidenced by a significantly higher proportion of polyploid cells in the TE as in the ICM (IWASAKI et al., 1992; VIUFF et al., 2002). The threshold of 27 h after IVF for completion of the first cleavage resulted in a significantly decreased blastocyst rate by day 7 when compared to non-sorted embryos. This indicates that embryos with an increased frequency of blastomeres with errors in the chromosomal setup were successfully selected applying above-mentioned parameter.

When comparing the chimera aggregation techniques, a highly increased blastocyst rate when using PHA was recorded. The development of chimeras was observed using time lapse microscopy and chimeras aggregated with PHA tightly compacted to one single morula before developing the blastocoel cavity while compaction prior to blastocyst development was not visible that clearly in chimeras produced by the sandwich technique (see Figure 8). Additionally, integration of the donor blastomeres differed between aggregation techniques with PHA-chimeras showing a higher contribution of eGFP positive blastomeres to the ICM than sandwich-chimeras (40% vs. 16%, $p<0.05$). Fixing the donor blastomeres in between the host embryos might direct them to the inside of the chimeric aggregate and favor ICM lineage commitment of the donor blastomeres. Because although the spatial context of a blastomere is not the only factor that defines its later commitment to a lineage, cells located on the inside of a morula are inclined to colonize the ICM (PFEFFER, 2014).

Using CLSM and immunofluorescent differential staining with a TE specific factor (CDX2), it was possible to accurately determine the total cell number and the number of TE-cells in aggregation chimeras with wild-type host embryos.

Unsurprisingly, the total cell number of chimeras exceeds the total cell number of control embryos. Nevertheless, considering the double cell number after aggregation, the difference is not marked. This brings up the question whether embryos have a certain mechanism to avoid excessive cell numbers before implantation to ensure normal development. The number of cells in the ICM of chimeras was increased when compared to control embryos; however, there were no significant differences between the groups in the ICM/total cell number ratio (see Table 7). Therefore, chimeras in this experiment had a normal ICM/TE ratio with functional cell lineages, shown by the positive, respectively negative staining of TE and ICM with the CDX2 antibody. Interestingly, BANG et al. (2015) found contradicting results after aggregation of three day 3 transgenic morulae derived from SCNT. On day 8 of development, blastocysts derived by embryo aggregation had a threefold higher total cell number when compared to non-aggregated SCNT blastocysts. In addition, the increase was mainly due to a highly elevated number of TE cells resulting in a very low ICM/TE ratio of 1:4.8, whereas in this study, a slight increase in number of ICM cells was recorded. These data suggest that embryos from SCNT may react differently to aggregation then *in vitro* produced embryos. Evaluation of cell numbers in PHA treated and handling control embryos showed that ZP removal and PHA treatment had no significant effect.

CLSM analysis of chimeras with wild-type host embryos confirmed that blastomeres from day 5 morulae are able to colonize the ICM when aggregated to day 4 host morulae. This enables the use of *ex vivo* derived embryos flushed from the uterus for multiplication via chimeric complementation, which bares many advantages. More cells are available, so more chimeras may be aggregated per donor embryo while enough cells are still available for simultaneous genotyping (PONSART et al., 2014). Also, in comparison to a study by HIRIART et al. (2013), who used day 3 donor and day 2 host embryos, blastocyst rates were highly increased with day 5 donor and day 4 host embryos. Chimera production is probably improved, because at this developmental stage embryonic genome activation is already complete and embryos selected for aggregation do not suffer from developmental block (MEIRELLES et al., 2004; GRAF et al., 2014). CLSM also showed that none of the chimeras had exclusive ICM colonization by donor blastomeres and when integrated to the ICM,

they only represented a small portion of the pluripotent cell line (Table 8), indicating that only two donor blastomeres are too few to build a major part of the ICM. Additionally, CLSM revealed that chimera evaluation only by epifluorescence microscopy (Figure 7) is not reliable regarding the site and quality of donor blastomere integration. For example, the ICM of the chimera in Figure 9 would appear as fully colonized by eGFP positive blastomeres in epifluoresence microscopy. Nevertheless, a 3D projection of confocal sections of the chimera reveals that only few eGFP cells are found at the edge of the ICM and even seem to be developing into the hypoblast, which later forms the primitive yolk sac and does not contribute to the embryo proper (MADDOX-HYTTEL et al., 2003). Evaluation of such chimeras with epifluorescence microscopy would lead to false positive results regarding successful integration of donor blastomeres to the ICM and consequently the multiplication of a desired genotype, which in a species like cattle with long gestation periods and costly housing is not acceptable.

OCT4 has no influence on the first lineage differentiation but KO embryos fail during the second lineage differentiation due to loss of NANOG

To generate embryos with a KO of *OCT4*, somatic cells were transfected with CRISPR/Cas9. Cas9 is directed to the *OCT4* locus by a specific sgRNA, where it induces a DSB. The error prone repair mechanism NHEJ then possibly leads to indels, which induce a shift in the reading frame of the gene and thus destroy its function. After screening 156 single cell clones, 4 (2.6%) showed mutation events of which only 1 clone carried a biallelic deletion that would induce a KO. Reported targeting efficiencies of CRISPR/Cas9 in somatic cells of domestic animals vary broadly with 9-70% in goat (NI et al., 2014) and 2.8-18% in pig (WHITWORTH et al., 2014) intending the KO of a gene and 32.2-80% in a gene knockin study with bovine cells (JEONG et al., 2016). In aforementioned studies, the high variation in efficiency relates to different cell lines (JEONG et al., 2016), the design of sgRNAs (WHITWORTH et al., 2014) or the targeting of different genes (NI et al., 2014). Therefore, a low CRISPR/Cas9 efficiency may be improved by testing different sgRNAs and cell lines, which was omitted in this study because the primary goal of producing a cell clone with a non-functional *OCT4* gene was achieved with the first transfection. Interestingly, mutation frequency was highly increased at the *ETF1* off-

target site (36%), which may be due to a less condensed chromatin status when compared to *OCT4*. In mouse thymocytes, the histones H3 and H4 of *Oct4* are hypoacetylated and lysine 4 of H3 (H3K4) is demethylated, leading to a silenced and condensed gene (KIMURA et al., 2004), while in pluripotent cells *Oct4* is packaged with acetylated H3/H4 and H3K4 is methylated (CEDAR & BERGMAN, 2009). This leads to the assumption, that also in the somatic cell line *WalterBF-Tg(PGK-EGFP)* used for transfection in this study, the *OCT4* locus was condensed. With the protein encoded by *ETF1* playing an essential role in termination of mRNA translation (KISSELEV et al., 2003), it is reasonable to suggest that it is active and therefore less condensed than *OCT4* in all cell types. ISAAC et al. (2016) have shown, that action of Cas9 decreases with DNA packaged on nucleosomes and that chromatin remodelers can enhance Cas9 activity, which shows that CRISPR/Cas9 efficiency is influenced by the chromatin status of the target gene. This interaction between targeting efficiency and chromatin status might explain the increased frequency of mutation events at the *ETF1* locus when compared to *OCT4*.

To study the role of OCT4 in bovine preimplantation development, embryos were reconstructed via SCNT from the above-mentioned cell clone (*OCT4* KO) and from non-transfected cells of the same source as a control (NT CTRL). Despite the fusion rate of the enucleated oocyte with the donor cell, there were no differences in development between embryos reconstructed from *OCT4* KO or NT CTRL cells until day 5 morula stage. The increased fusion rate with *OCT4* KO cells might be due to an enlarged cell size when compared to cells from NT CTRL (data not shown), which facilitates contact between somatic cell and oocyte while applying the electric pulse for fusion. The development to blastocyst stage by day 7 was strongly decreased in *OCT4* KO embryos when compared to NT CTRL (16.78 ± 10.21% vs. 32.07 ± 10.84%) and typically, blastocyst rate after SCNT varies between 20-60% (TSUNODA et al., 2006). It remains unclear if this effect on developmental competence is related to the loss of OCT4 or to a cell clone specific artefact. It is known from several studies in mouse, that the loss of maternal and zygotic OCT4 does not affect the number of homozygous *Oct4* null blastocysts in the litters from heterozygously floxed *Oct4* crosses, which remains at a Mendelian frequency of ~ 25% (NICHOLS et al., 1998; FRUM et al., 2013; WU et al., 2013; LE BIN et al.,

2014). Considering that *Oct4* has no effect on blastocyst rate in mouse, the decreased developmental competence of bovine *OCT4* KO embryos might be specific to the cell clone used in this study. Because besides inducing the biallelic deletion in the *OCT4* gene, CRISPR/Cas9 also caused a mutation in *ETF1*. This off-target effect may decrease the blastocyst rate, although the mutation only consists of a single nucleotide on one allele and is located in the first intron of *ETF1*. In addition, the procedures involved in producing mutated single cell clones, which include transfection and single cell culture followed by many passages, can alter the cells' properties. To examine the effect of both, the mutation in *ETF1* and the cell culture procedures, a single cell clone with the exact same mutation in *ETF1* and none in *OCT4* from the same transfection experiment was identified (*ETF1mut*^{2F11tm1}) and SCNT was performed. Unfortunately, results are inconclusive, as there was no significant difference in blastocyst rate, neither to *OCT4* KO nor to NT CTRL embryos. Therefore, from this data it is impossible to conclude whether the decreased blastocyst rate in *OCT4* KO embryos is a cell clone specific effect or due to the loss of OCT4.

At day 7, there was no difference in morphology between *OCT4* KO and NT CTRL embryos (Figure 13) and also none in the number of total cells (Table 10). This is in concordance to mouse *Oct4* KO embryos, where day 3.5 (NICHOLS et al., 1998) or day 3.75 (FRUM et al., 2013) blastocysts also have no reduced total cell count. These developmental stages are equivalent to bovine day 7 and 8, i.e. blastocyst stage and beginning of hypoblast differentiation, respectively. While there was no difference in total cell number between embryos from nuclear transfer experiments at day 7, IVP CTRL embryos had an increased total cell count. KOO et al. (2002) reported no difference in total cell number between embryos from IVP and SCNT at day 7, whereas various studies did find an increased cell count in IVP embryos (SONG et al., 2011; BANG et al., 2015; CHEN et al., 2015). This indicates, although data from the literature is contradicting, that bovine SCNT embryos tend to have a generally lower cell count than IVP embryos and that the difference in this study is not related to the cells used for SCNT. By day 9, *OCT4* KO embryos showed a marked decrease in size and total cell number when compared to controls. This is also reported for mouse day 4.25 *Oct4* KO blastocysts (the developmental equivalent

to bovine day 9), where TE cells proliferated less than in controls and growth of ICM cells stagnated (FRUM et al., 2013). Differential staining of TE and ICM with the TE-specific marker CDX2 showed that day 7 *OCT4* KO embryos have an unchanged percentage of TE cells when compared to NT CTRL and IVP CTRL embryos. Also, like in mouse day 3.5 blastocysts (WU et al., 2016), ICM cells did not stain positive for CDX2. This leads to the conclusion, that OCT4 is not required for the quantitative allocation of cells to either ICM or TE during the first lineage differentiation and that OCT4 does not repress CDX2 expression in the ICM. Therefore, other factors than OCT4 control the first differentiation event in bovine early preimplantation embryos and loss of OCT4 does not compromise the lineage segregation into ICM and TE, which coincides with the mouse *Oct4* KO model.

To confirm the absence of OCT4, embryos were subjected to immunofluorescent labeling of the protein. In control embryos (NT CTRL and IVP CTRL), OCT4 was expressed in all cells at day 5 morula stage. KHAN et al. (2012) reported that OCT4 is not detectable in earlier stages, i.e. from oocyte until 8-cell stage. At the 16-cell stage, when embryonic genome activation (EGA) is complete, they found a slight signal and strong signals were only detectable from day 5 morula onward. Interestingly, *OCT4* KO morulae at day 5 still expressed OCT4, albeit not in all nuclei and with decreased intensity. As embryonic *OCT4* is non-functional, the detected OCT4 must have derived from maternal stores of the protein or mRNA in the oocyte. By day 7, all cells stained negative for OCT4 in *OCT4* KO embryos, so maternal OCT4 had completely decayed, while control embryos ubiquitously expressed OCT4. With the NT CTRL embryos showing the same OCT4 expression pattern as the IVP CTRLs, i.e. expression in the ICM and co-expression with CDX2 in the TE as reported previously (BERG et al., 2011), any effects of SCNT on timing and localization of OCT4 expression can be excluded.

As mentioned above, expression of CDX2 at day 7 blastocyst stage was not affected by *OCT4* KO. At day 5 morula stage, CDX2 was expressed in the cytoplasm and subsequently migrated to the nuclei of TE cells in all embryos. MADEJA et al. (2013) performed immunofluorescent stainings against CDX2 using the same antibody as in this study and found cytoplasmic expression until compacted morula stage, when CDX2 was also detected in the nuclei. Transition of CDX2 from

cytoplasm to nucleus is therefore most likely to occur during compaction, as day 5 morulae examined here were not compacted yet. Another study reports no cytoplasmic expression and first detection of CDX2 at blastocyst stage when using an antibody with a different epitope (GOISSIS & CIBELLI, 2014), indicating that different isoforms of CDX2 may be present during preimplantation development and that further examination of the temporal and spatial expression of CDX2 in bovine is necessary.

As developmental failure of *Oct4* KO mouse embryos is connected to their inability to complete the second lineage differentiation (FRUM et al., 2013; LE BIN et al., 2014), epiblast (EPI) and hypoblast (HB) segregation was observed in bovine *OCT4* KO embryos. By staining against the EPI and HB specific markers NANOG and GATA6 at days 5, 7 and 9, it was possible to determine the spatial and temporal expression patterns and to examine the effect of loss of OCT4 on the segregation of the second differentiated lineage (HB) and on the maintenance of the pluripotent EPI. At day 5 morula stage, NANOG and GATA6 co-expressed in the majority of cells, while in *OCT4* KO embryos the percentage of GATA6 positive cells was significantly decreased. Reports on NANOG expression at morula stage are not consistent in the literature, e.g. KUIJK et al. (2012) reported no expression, KHAN et al. (2012) expression in the nucleolus and MADEJA et al. (2013) detected signals in the cytoplasm and rings around and the nuclei. When comparing results, it is important to take into account the exact developmental stage. Unfortunately, only KUIJK et al. (2012) further specified their material by stating the total cell count at time of examination (day 5) with 19.7 ± 6.9 while here it was 56.1 ± 12 in IVP CTRL embryos, without significant difference to embryos from SCNT. With increasing cell count at day 6 (39 ± 18.9), KUIJK et al. (2012) also found ubiquitous weak expression of NANOG. GRAF et al. (2014) determined the 8-cell stage as onset of embryonic *NANOG* transcription and found transcripts in all developmental stages until blastocyst stage. Additionally, blastomeres of mouse morulae also express NANOG before forming the blastocyst (CHAZAUD et al., 2006), therefore data from the literature make the results presented here plausible. Reports on GATA6 expression in bovine morulae are scarce, however KUIJK et al. (2012) found the same pattern at day 6 with most nuclei staining positive. No data on NANOG and

GATA6 expression are available from the mouse *Oct4* KO models at morula stage, which makes it difficult to speculate, why the percentage of GATA6 positive blastomeres in *OCT4* KO morulae was significantly decreased.

At day 7, a salt and pepper distribution of NANOG and GATA6 was already visible within the ICM of control embryos. Nevertheless, expression was not yet mutually exclusive and cells from the TE still stained positive for both markers. The same staining pattern for NANOG and GATA6 in day 7 bovine blastocysts has been reported previously (KHAN et al., 2012; KUIJK et al., 2012; DENICOL et al., 2014). Remarkably, *OCT4* KO embryos did not express any NANOG by day 7, but still contained cells that stained positive for GATA6 in a similar pattern as in the controls. This is especially interesting in the light of the disturbed second lineage differentiation in mouse *Oct4* KO embryos, where ICM cells at day 3.5-3.75 still show the same distribution of EPI and primitive endoderm (PE, the equivalent to bovine hypoblast) precursor cells. At day 4.25, the ICM contains no more GATA6 positive cells but NANOG is still present (FRUM et al., 2013; LE BIN et al., 2014), which is completely opposite to the bovine *OCT4* KO phenotype observed in this study. In mouse, the current working model of PE differentiation (Figure 3) states, that OCT4 regulates FGF4 expression to induce PE cell fate and additionally activates PE genes in PE precursor cells (FRUM et al., 2013). In bovine blastocysts depleted of FGF4 signaling, GATA6 expression is still maintained and therefore not FGF4 dependent (KUIJK et al., 2012), which might explain the unchanged expression of GATA6 in *OCT4* KO day 7 blastocysts. NANOG expression at morula stage is unchanged in *OCT4* KO embryos and also derived from *de novo* transcripts, as there are no maternal *NANOG* mRNA stores in the oocyte (GRAF et al., 2014) and the half-life of NANOG protein is ~ 3 h in mouse and human embryonic stem cells (HAYASHI et al., 2015). This suggests that initiation of NANOG expression and maintenance until morula stage is not OCT4 dependent, but during the first lineage differentiation NANOG is lost, so its expression in the ICM and therefore EPI maintenance requires OCT4.

By day 9, *OCT4* KO embryos had also lost GATA6 expression, while in controls expression of EPI and HB markers was limited to the ICM and mutually exclusive. Unfortunately, embryos cultured *in vitro* until day 9 had many degenerated nuclei,

which made further analysis of differentiation events futile. Mouse embryos are flushed from the uterus at any time point before implantation, i.e. until day 4.25, when PE differentiation is already complete (NAGY et al., 2003). To be able to thoroughly study the effects of *OCT4* KO on the second lineage differentiation in bovine embryos, day 9 embryos need to be produced without artefacts from *in vitro* culture, which can be achieved by either improving culture conditions or by transfer of embryos to recipients and flushing them non-surgically at day 9. This would provide authentic material to investigate the mechanisms during second lineage differentiation, which apparently differ substantially from the lessons learned with the mouse model. Knowledge about the interactions between the transcription factors that regulate pluripotency and first differentiation events might also help understand, why the establishment of embryonic stem cell lines in bovine is still unsuccessful. Additionally, human preimplantation development resembles bovine more than mouse in many aspects, i.e. the interaction between OCT4 and CDX2 (BERG et al., 2011) and the role of FGF4/MAPK signaling (KUIJK et al., 2012; ROODE et al., 2012), which might render bovine preimplantation embryos the better model to study human development.

Wild-type donor blastomeres do not populate the ICM in chimeras with *OCT4* KO host embryos

To test the hypothesis that due to their deficient pluripotency network, cells from an *OCT4* KO host embryo differentiate into extraembryonic tissues while wild-type donor blastomeres populate the ICM within a chimera, two day 4 *OCT4* KO host morulae were subjected to synchronic aggregation with four blastomeres from a wild-type morula. Blastocyst rate of aggregated chimeras markedly increased when compared to single *OCT4* KO embryos (74% vs. 17%, respectively), showing a positive effect of aggregation on development as shown before in bovine embryos from SCNT (BANG et al., 2015). The developmental kinetics did not change and chimeras without OCT4 showed compaction of the aggregation partners to one single morula before development of the blastocoel, suggesting that these mechanisms are independent of OCT4. Nevertheless, chimeras with *OCT4* KO hosts had expanded less 96 h after aggregation when compared to wild-type chimeras, which is analog to single day 9 hatched *OCT4* KO blastocyst.

Developed blastocysts were stained against OCT4 and CDX2 and analyzed using CLSM. In 7 out of 13 blastocysts, donor blastomeres integrated to the chimera and surprisingly mainly differentiated into TE cells, while cells from the *OCT4* KO hosts were found in the ICM of every analyzed blastocyst. In asynchronic wild-type chimeras, the percentage of blastocysts with donor cells in the TE was only 1.2%, showing a clear tendency of the developmentally advanced donor cells towards the ICM. With *OCT4* KO hosts, embryos were subjected to synchronic aggregation to study the effect of an OCT4 deficiency on lineage segregation; therefore, data from the two experiments are not comparable. However, HIRIART et al. (2013) compared synchronic and asynchronic aggregation and found a higher contribution of donor cells to the ICM in the latter, suggesting that the developmental stages of host and donor influence their lineage allocation and that contribution of donor cells to the ICM could also be improved in *OCT4* KO chimeras using developmentally advanced donor cells. Nevertheless, loss of OCT4 did not drive the host embryos into TE differentiation, once again stretching the embryo's independence from OCT4 during the first lineage segregation. By injection of embryonic stem cells (ESCs) to 8-cell stage mouse embryos, fetuses completely derived from ESCs can be produced, because the injected cells colonize the ICM (POUEYMIROU et al., 2007). FRUM et al. (2013) injected ESCs to *Oct4* KO mouse embryos to examine, if the wild-type cells can rescue the *Oct4* KO phenotype. In these chimeras, contribution of ESCs did not differ between wild-type and *Oct4* KO hosts and the donor cells colonized the ICM. Therefore, in mouse, allocation of donor and host to the cell lineages in the chimeric blastocyst is not affected by a OCT4 deficient host. The experiments also showed, that OCT4 is required cell-autonomously for the second lineage differentiation of the primitive endoderm, which is why the injected ESCs were not able to rescue the *Oct4* KO phenotype. It remains unclear, why the wild-type blastomeres in bovine *OCT4* KO chimeras mainly contributed to the TE. Further experiments are necessary to evaluate the effects of synchronic vs. asynchronic aggregation and additionally, stochastic effects at the first lineage differentiation are to be excluded by aggregation of an equal amount of wild-type and *OCT4* KO cells. Also, by aggregation of previously disaggregated *OCT4* KO and wild-type blastomeres, random position inside or outside the chimeric morula can be ensured

and bias in allocation to the TE or ICM resulting from the former location in the morula is prevented. Given this additional data, it may be possible to clarify whether differentiation of wild-type blastomeres to TE cells in *OCT4* KO chimeras is due an unknown mechanism involving TE differentiation and OCT4, or if the effects seen here are of different nature. The clear and stable eGFP expression of cells derived from the *OCT4* KO hosts makes the established system perfect for further investigations.

The approach to use *OCT4* KO embryos in a biotechnological context to multiply elite embryos is fruitless, because aggregation with a few wild-type cells did not have the anticipated effect, that those cells would primarily colonize the ICM and give rise to the embryo proper. Although it is ensured that the *OCT4* KO hosts lose all pluripotency due to the loss of NANOG at day 7 and therefore are not capable of contribution to the fetus, donor cells integrated poorly to the ICM and furthermore predominantly differentiated to TE cells. The approach presented also includes SCNT for the production of the *OCT4* KO hosts, because this is the only possible way to provide definite *OCT4* KO embryos before aggregation. Injection of CRISPR/Cas9 to zygotes would be a technically less demanding alternative, but until now there is no possibility to monitor if *OCT4* was knocked out before aggregating the chimera. Therefore, multiplication of embryos using chimeric complementation with *OCT4* KO host embryos is neither efficient nor technically undemanding.

VI. Summary

Chimeric bovine embryo multiplication with *OCT4* knockout host embryos

With the advent of genomic selection and the possibility to select superior genotypes on the embryonic level, the commercial value of individual embryos has increased and therefore, the multiplication of elite bovine embryos is of great interest. Available techniques, like embryonic cell nuclear transfer or blastomere separation to produce monozygotic twins, have not been implemented due to high technical demand or low efficiencies. The multiplication of elite embryos by the production of aggregation chimeras is based on the concept that few blastomeres of a donor embryo form the inner cell mass (ICM), whereas host embryo cells preferentially contribute to the trophectoderm (TE). Later in development, cells from the ICM will give rise to the fetus, while TE cells form the embryonic part of the placenta, so resulting offspring exclusively carries the donor's genotype. The biggest challenge in this technique is to find ways to exclude host embryo cells from the ICM in the chimeric blastocyst, while potential advantages are a high efficiency regarding transferable blastocysts and a low technical demand.

In this thesis, I first tested wild-type embryos that did not complete their first cleavage until 27 h after fertilization as host embryos and additionally evaluated the effect of phytohemagglutinin (PHA), a membrane protein binding agent, on the development of aggregation chimeras. The use of PHA highly increased the blastocyst rate and enabled stable positioning of the aggregation partners within the chimera. This increased the integration of donor blastomeres to the ICM, probably because their position was fixed in between the host embryos so they eventually migrated to the inside of the emerging morula, where they are more likely to contribute to the ICM. Nevertheless, this approach did not provide sufficient segregation of donor and host into the different cell lineages to be suitable for the multiplication of genetically valuable embryos.

The rationale to use an *OCT4* knockout (KO) embryo as host in chimeric multiplication was to ensure its absolute exclusion from potential offspring. OCT4 is on top of the pluripotency hierarchy and OCT4 deficient blastomeres from the host

embryo cannot maintain their pluripotent state and thus do not contribute to the embryo proper, but form extraembryonic tissues to support the few donor cells. To test this hypothesis, *OCT4* was knocked out in somatic cells using CRISPR/Cas9 and embryos were subsequently reconstructed with somatic cell nuclear transfer. Because this is, to my knowledge, the first report on *OCT4* KO in bovine embryos, the KO phenotype was examined before performing chimera aggregation experiments. In conclusion, *OCT4* KO does not affect the total cell number or quantitative allocation of cells to ICM or TE by day 7 blastocyst stage, but the epiblast specific marker NANOG is already lost. This is in contrast to the development of mouse *Oct4* KO embryos, where NANOG expression is maintained, indicating substantial differences between mouse and bovine in the regulation of the second lineage differentiation.

In chimeras from *OCT4* KO host embryos and wild-type donor cells, the donor cells did not, as anticipated, colonize the ICM, but predominantly differentiated into TE cells. It remains unclear why the wild-type blastomeres in bovine *OCT4* KO chimeras mainly contributed to the TE and if there is an underlying mechanism involving TE differentiation and OCT4 that caused the wild-type cells to mainly contribute to this lineage. In conclusion, the KO of *OCT4* would exclude the hosts' cells from the embryo proper due to the early loss of NANOG, but the poor contribution of donor cells to the ICM of the chimeras makes the proposed method for multiplication of elite embryos infeasible.

VII. Zusammenfassung

Multiplikation von Rinderembryonen durch Chimärenbildung mit *OCT4* knockout Embryonen

Mit dem Aufkommen der genomischen Selektion und der Möglichkeit züchterisch wertvolle Genotypen bereits im embryonalen Stadium zu identifizieren, ist der kommerzielle Wert einzelner Embryonen gestiegen, weshalb die Multiplikation von Rinderembryonen von großem Interesse ist. Bereits verfügbare Methoden wie z.B. Kerntransfer embryonaler Zellen oder das Zerteilen von Embryonen, um monozygote Zwillinge zu produzieren, werden derzeit wegen ihrem hohen technischen Anspruch oder geringer Effizienz nicht durchgeführt. Die Multiplikation wertvoller Embryonen mittels Chimären-Aggregation beruht auf der Idee, dass wenige Zellen dieser Embryonen, sog. Spenderzellen, die innere Zellmasse (inner cell mass, ICM) bilden, während Empfängerembryonen das Trophektoderm (TE) bilden. In der weiteren Entwicklung entsteht der Fötus aus den Zellen der ICM und das TE entwickelt sich weiter zum embryonalen Bestandteil der Plazenta, so dass Nachkommen ausschließlich den Genotyp des positiv selektierten Embryos tragen. Die größte Herausforderung bei dieser Methode besteht darin, Wege zu finden, Empfängerembryonen von der ICM auszuschließen. Die Vorteile liegen bei einer hohen Effizienz hinsichtlich übertragbarer Embryonen und einem geringen technischen Anspruch.

In dieser Arbeit wurden zuerst Wildtyp-Embryonen, die ihre erste Zellteilung nicht vor 27 h nach Befruchtung abgeschlossen hatten, als Empfängerembryonen getestet. Zusätzlich wurde der Einsatz von Phytohämagglutinin (PHA), ein Mittel das Membranproteine aneinander bindet, bei der Aggregation der Embryonen geprüft. Mit PHA konnte die Blastozystenrate erheblich gesteigert werden, außerdem wurden die Positionen der Aggregationspartner in der Chimäre nachhaltig bestimmt. Dadurch wurde die Integration von Spenderzellen in die ICM erhöht, was möglicherweise darauf zurückzuführen ist, dass die Spenderzellen zwischen den Empfängerembryonen platziert wurden. In der Morula, die nach Aggregation entsteht, befanden sich die Spenderzellen dann eventuell im Inneren, was die

Wahrscheinlichkeit sich zur ICM zu entwickeln verbessert. Nichtsdestotrotz ergab sich bei dieser Methode nicht genügend Trennung zwischen Spender- und Empfängerzellen, so dass sich Empfängerzellen noch immer in der ICM befanden. Dadurch ist diese Multiplikationsmethode für genetisch wertvolle Embryonen ungeeignet.

Um auf sichere Art und Weise Empfängerembryonen von der ICM auszuschließen, wurden Empfängerembryonen mit einem ausgeschalteten *OCT4* Gen hergestellt (*OCT4* knockout, KO). *OCT4* steht an der Spitze der Pluripotenzregulation, weshalb Zellen mit einem *OCT4* KO ihre Pluripotenz nicht erhalten und so auch nicht Teil des entstehenden Embryos werden können. Vielmehr entwickeln sie extraembryonale Gewebe und unterstützen so die wenigen Zellen des Spenderembryos. Um diese Hypothese zu prüfen, wurde *OCT4* in somatischen Zellen mittels CRISPR/Cas9 ausgeschaltet, um dann durch somatischen Zellkerntransfer *OCT4* KO Embryonen herzustellen. Bislang ist das die erste Studie, die den Effekt eines *OCT4* KO bei Rinderembryonen untersucht, weshalb vor den Aggregationsexperimenten der Phänotyp dieser Embryonen beschrieben wurde. Zusammenfassend hat ein *OCT4* KO weder Einfluss auf die Gesamtzellzahl noch auf die Zellzahlen der ICM oder des TE in der Blastozyste am Tag 7 der Entwicklung. Jedoch ist in diesem Stadium der Epiblast spezifische Marker NANOG nicht mehr vorhanden. Dies steht im Gegensatz zur Entwicklung von Maus *Oct4* KO Embryonen, bei denen die Expression von NANOG erhalten bleibt. Dies zeigt wiederum grundlegende Unterschiede zwischen den Spezies während der zweiten Zelldifferenzierung auf.

In den Chimären, die aus *OCT4* KO Embryonen und Wildtyp-Spenderzellen hergestellt wurden, bestand die ICM nicht wie erwartet aus Spenderzellen, sondern differenzierten hauptsächlich zu Zellen des TE. Die Gründe für diese Entwicklung sind unbekannt; auch die Frage, ob es einen zugrundeliegenden Mechanismus gibt, der OCT4 und die Entstehung des TE beinhaltet und diese Differenzierung verursacht, bleibt ungeklärt. Grundsätzlich würde ein *OCT4* KO die Beteiligung der Empfängerembryonen am Fötus durch den frühen Verlust von NANOG verhindern, allerdings macht die ungenügende Besiedelung der ICM durch Spenderzellen die Durchführung dieser Embryomultiplikationsmethode unmöglich.

VIII. Index of Tables

IX. Index of Figures

X. References

Akagi S, Yamaguchi D, Matsukawa K, Mizutani E, Hosoe M, Adachi N, Kubo M, Takahashi S. Developmental ability of somatic cell nuclear transferred embryos aggregated at the 8-cell stage or 16-to 32-cell stage in cattle. Journal of Reproduction and Development 2011; 57: 500-6.

Anderson D, Billingham RE, Lampkin GH, Medawar PB. The use of skin grafting to distinguish between monozygotic and dizygotic twins in cattle. Heredity 1951; 5: 379-97.

Bang JI, Jin JI, Ghanem N, Choi BH, Fakruzzaman M, Ha AN, Lee KL, Uhm SJ, Ko DH, Koo BC, Lee JG, Kong IK. Quality improvement of transgenic cloned bovine embryos using an aggregation method: effects on cell number, cell ratio, embryo perimeter, mitochondrial distribution, and gene expression profile. Theriogenology 2015; 84: 509-23.

Berg DK, Smith CS, Pearton DJ, Wells DN, Broadhurst R, Donnison M, Pfeffer PL. Trophectoderm lineage determination in cattle. Developmental cell 2011; 20: 244-55.

Brem G, Tenhumberg H, Kräußlich H. Chimerism in cattle through microsurgical aggregation of morulae. Theriogenology 1984; 22: 609-13.

Callaway E (2016) UK scientists gain licence to edit genes in human embryos. In: Nature. 18-

Cedar H, Bergman Y. Linking DNA methylation and histone modification: patterns and paradigms. Nature Reviews Genetics 2009; 10: 295-304.

Cenariu M, Pall E, Cernea C, Groza I. Evaluation of bovine embryo biopsy techniques according to their ability to preserve embryo viability. Journal of Biomedicine and Biotechnology 2012; 2012: 1-5.

Chazaud C, Yamanaka Y, Pawson T, Rossant J. Early lineage segregation between epiblast and primitive endoderm in mouse blastocysts through the Grb2-MAPK pathway. Developmental cell 2006; 10: 615-24.

Chazaud C, Yamanaka Y. Lineage specification in the mouse preimplantation embryo. Development 2016; 143: 1063-74.

Chen H, Zhang L, Guo Z, Wang Y, He R, Qin Y, Quan F, Zhang Y. Improving the development of early bovine somatic-cell nuclear transfer embryos by treating adult donor cells with vitamin C. Molecular reproduction and development 2015; 82: 867-79.

Cibelli JB, Stice SL, Golueke PJ, Kane JJ, Jerry J, Blackwell C, Ponce de Leon FA, Robl JM. Transgenic bovine chimeric offspring produced from somatic cell-derived stem-like cells. Nature biotechnology 1998; 16: 642-6.

Cotterman C. Somatic mosaicism for antigen A2. Human Heredity 1956; 6: 520-1.

Crispo M, Mulet A, Tesson L, Barrera N, Cuadro F, dos Santos-Neto P, Nguyen T, Crénéguy A, Brusselle L, Anegón I. Efficient generation of myostatin knock-out sheep using CRISPR/Cas9 technology and microinjection into zygotes. PloS one 2015; 10: e0136690.

Curnow E, Gunn I, Trounson A. Electrofusion of two-cell bovine embryos for the production of tetraploid blastocysts in vitro. Molecular reproduction and development 2000; 56: 372-7.

De Chaumont F, Dallongeville S, Chenouard N, Hervé N, Pop S, Provoost T, Meas-Yedid V, Pankajakshan P, Lecomte T, Le Montagner Y. Icy: an open bioimage informatics platform for extended reproducible research. Nature methods 2012; 9: 690-6.

Denicol AC, Block J, Kelley DE, Pohler KG, Dobbs KB, Mortensen CJ, Ortega MS, Hansen PJ. The WNT signaling antagonist Dickkopf-1 directs lineage commitment and promotes survival of the preimplantation embryo. The FASEB Journal 2014; 28: 3975-86.

Du F, Shen P-c, Xu J, Sung L-Y, Jeong B, Lucky Nedambale T, Riesen J, Cindy Tian X, Cheng WT, Lee S-N. The cell agglutination agent, phytohemagglutinin-L, improves the efficiency of somatic nuclear transfer cloning in cattle *Bos taurus*. Theriogenology 2006; 65: 642-57.

Eakin GS, Behringer RR. Tetraploid development in the mouse. Developmental Dynamics 2003; 228: 751-66.

Frum T, Halbisen MA, Wang C, Amiri H, Robson P, Ralston A. Oct4 cell-autonomously promotes primitive endoderm development in the mouse blastocyst. Developmental cell 2013; 25: 610-22.

Fujita T, Umeki H, Shimura H, Kugumiya K, Shiga K. Effect of group culture and embryo-culture conditioned medium on development of bovine embryos. The Journal of reproduction and development 2006; 52: 137-42.

Gaj T, Gersbach CA, Barbas CF. ZFN, TALEN, and CRISPR/Cas-based methods for genome engineering. Trends in Biotechnology 2013; 31: 397-405.

Goissis MD, Cibelli JB. Functional characterization of CDX2 during bovine preimplantation development in vitro. Molecular reproduction and development 2014; 81: 962-70.

Graf A, Krebs S, Zakhartchenko V, Schwalb B, Blum H, Wolf E. Fine mapping of genome activation in bovine embryos by RNA sequencing. Proceedings of the National Academy of Sciences 2014; 111: 4139-44.

Hai T, Teng F, Guo R, Li W, Zhou Q. One-step generation of knockout pigs by zygote injection of CRISPR/Cas system. Cell research 2014; 24: 372.

Hall TA (1999) BioEdit: a user-friendly biological sequence alignment editor and analysis program for Windows 95/98/NT. Nucleic acids symposium series. 95-8

Hayashi Y, Caboni L, Das D, Yumoto F, Clayton T, Deller MC, Nguyen P, Farr CL, Chiu H-J, Miller MD. Structure-based discovery of NANOG variant with enhanced properties to promote self-renewal and reprogramming of pluripotent stem cells. Proceedings of the National Academy of Sciences 2015; 112: 4666-71.

Hayes B, Bowman P, Chamberlain A, Goddard M. Genomic selection in dairy cattle: progress and challenges. Journal of dairy science 2009; 92: 433-43.

Heigwer F, Kerr G, Boutros M. E-CRISP: fast CRISPR target site identification. Nature methods 2014; 11: 122-3.

Heo YT, Quan X, Xu YN, Baek S, Choi H, Kim N-H, Kim J. CRISPR/Cas9 nuclease-mediated gene knock-in in bovine-induced pluripotent cells. Stem cells and development 2014; 24: 393-402.

Herr W, Cleary MA. The POU domain: versatility in transcriptional regulation by a flexible two-in-one DNA-binding domain. Genes Dev 1995; 9: 1679-93.

Hiendleder S, Mund C, Reichenbach H-D, Wenigerkind H, Brem G, Zakhartchenko V, Lyko F, Wolf E. Tissue-specific elevated genomic cytosine methylation levels are associated with an overgrowth phenotype of bovine fetuses derived by in vitro techniques. Biology of Reproduction 2004; 71: 217-23.

Hiriart MI, Bevacqua RJ, Canel NG, Fernández-Martín R, Salamone DF. Production of chimeric embryos by aggregation of bovine egfp eight-cell stage blastomeres with two-cell fused and asynchronic embryos. Theriogenology 2013; 80: 357-64.

Hofmann A, Zakhartchenko V, Weppert M, Sebald H, Wenigerkind H, Brem G, Wolf E, Pfeifer A. Generation of transgenic cattle by lentiviral gene transfer into oocytes. Biology of Reproduction 2004; 71: 405-9.

Hofmann A, Kessler B, Ewerling S, Kabermann A, Brem G, Wolf E, Pfeifer A. Epigenetic regulation of lentiviral transgene vectors in a large animal model. Molecular Therapy 2006; 13: 59-66.

Hsu PD, Lander ES, Zhang F. Development and applications of CRISPR-Cas9 for genome engineering. Cell 2014; 157: 1262-78.

Hyttel P, Sinowatz F, Vejlsted M, Betteridge K (2009) Essentials of domestic animal embryology. Elsevier Health Sciences

Isaac RS, Jiang F, Doudna JA, Lim WA, Narlikar GJ, Almeida R. Nucleosome breathing and remodeling constrain CRISPR-Cas9 function. eLife 2016; 5: e13450.

Iwasaki S, Kono T, Fukastu H, Nakahara T. Production of bovine tetrapolid embryos by electrofusion and their developmental capability in vitro. Gamete research 1989; 24: 261-7.

Iwasaki S, Hamano S, Kuwayama M, Yamashita M, Ushijima H, Nagaoka S, Nakahara T. Developmental changes in the incidence of chromosome anomalies of bovine embryos fertilized in vitro. Journal of Experimental Zoology 1992; 261: 79-85.

Iwasaki S, Campbell KH, Galli C, Akiyama K, Iwasaki S. Production of live calves derived from embryonic stem-like cells aggregated with tetraploid embryos. Biology of Reproduction 2000; 62: 470-5.

Jeong Y-H, Kim YJ, Kim EY, Kim SE, Kim J, Park MJ, Lee H-G, Park SP, Kang M-J. Knock-in fibroblasts and transgenic blastocysts for expression of human FGF2 in the bovine β-casein gene locus using CRISPR/Cas9 nuclease-mediated homologous recombination. Zygote 2016; 24: 442-56.

Kang L, Wang J, Zhang Y, Kou Z, Gao S. iPS cells can support full-term development of tetraploid blastocyst-complemented embryos. Cell Stem Cell 2009; 5: 135-8.

Kang M, Piliszek A, Artus J, Hadjantonakis A-K. FGF4 is required for lineage restriction and salt-and-pepper distribution of primitive endoderm factors but not their initial expression in the mouse. Development 2013; 140: 267-79.

Kehler J, Tolkunova E, Koschorz B, Pesce M, Gentile L, Boiani M, Lomelí H, Nagy A, McLaughlin KJ, Schöler HR. Oct4 is required for primordial germ cell survival. EMBO reports 2004; 5: 1078-83.

Khan DR, Dubé D, Gall L, Peynot N, Ruffini S, Laffont L, Le Bourhis D, Degrelle S, Jouneau A, Duranthon V. Expression of pluripotency master regulators during two key developmental transitions: EGA and early lineage specification in the bovine embryo. PloS one 2012; 7: e34110.

Kimura H, Tada M, Nakatsuji N, Tada T. Histone code modifications on pluripotential nuclei of reprogrammed somatic cells. Molecular and cellular biology 2004; 24: 5710-20.

Kirchhof N, Carnwath J, Lemme E, Anastassiadis K, Schöler H, Niemann H. Expression pattern of Oct-4 in preimplantation embryos of different species. Biology of Reproduction 2000; 63: 1698-705.

Kisselev L, Ehrenberg M, Frolova L. Termination of translation: interplay of mRNA, rRNAs and release factors? The EMBO Journal 2003; 22: 175-82.

Koo D-B, Kang Y-K, Choi Y-H, Park JS, Kim H-N, Oh KB, Son D-S, Park H, Lee K-K, Han Y-M. Aberrant allocations of inner cell mass and trophectoderm cells in bovine nuclear transfer blastocysts. Biology of Reproduction 2002; 67: 487-92.

Kuijk EW, van Tol LT, Van de Velde H, Wubbolts R, Welling M, Geijsen N, Roelen BA. The roles of FGF and MAP kinase signaling in the segregation of the epiblast and hypoblast cell lineages in bovine and human embryos. Development 2012; 139: 871-82.

Kurome M, Kessler B, Wuensch A, Nagashima H, Wolf E. Nuclear transfer and transgenesis in the pig. In: Nuclear Reprogramming: Springer 2015: 37-59.

Kurosaka S, Eckardt S, McLaughlin KJ. Pluripotent lineage definition in bovine embryos by Oct4 transcript localization. Biology of Reproduction 2004; 71: 1578-82.

Kwon J, Namgoong S, Kim N-H. CRISPR/Cas9 as Tool for Functional Study of Genes Involved in Preimplantation Embryo Development. PloS one 2014; 10: e0120501-e.

Lanner F, Rossant J. The role of FGF/Erk signaling in pluripotent cells. Development 2010; 137: 3351-60.

Le Bin GC, Muñoz-Descalzo S, Kurowski A, Leitch H, Lou X, Mansfield W, Etienne-Dumeau C, Grabole N, Mulas C, Niwa H. Oct4 is required for lineage priming in the developing inner cell mass of the mouse blastocyst. Development 2014; 141: 1001-10.

Leidenfrost S, Boelhauve M, Reichenbach M, Güngör T, Reichenbach H-D, Sinowatz F, Wolf E, Habermann FA. Cell arrest and cell death in mammalian preimplantation development: lessons from the bovine model. PloS one 2011; 6: e22121.

Maddox-Hyttel P, Alexopoulos N, Vajta G, Lewis I, Rogers P, Cann L, Callesen H, Tveden-Nyborg P, Trounson A. Immunohistochemical and ultrastructural characterization of the initial post-hatching development of bovine embryos. Reproduction 2003; 125: 607-23.

Madeja ZE, Sosnowski J, Hryniewicz K, Warzych E, Pawlak P, Rozwadowska N, Plusa B, Lechniak D. Changes in sub-cellular localisation of trophoblast and inner cell mass specific transcription factors during bovine preimplantation development. BMC developmental biology 2013; 13: 1-17.

Mali P, Yang L, Esvelt KM, Aach J, Guell M, DiCarlo JE, Norville JE, Church GM. RNA-guided human genome engineering via Cas9. Science 2013; 339: 823-6.

Mallikarjunan N, Marathe S, Rajalakshmi D, Mahesh S, Jamdar S, Sharma A. Effect of ionizing radiation on structural and functional attributes of red kidney bean *Phaseolus vulgaris* lectin. LWT-Food Science and Technology 2014; 59: 300-7.

Meirelles F, Caetano A, Watanabe Y, Ripamonte P, Carambula S, Merighe G, Garcia S. Genome activation and developmental block in bovine embryos. Animal Reproduction Science 2004; 82: 13-20.

Messinger SM, Albertini DF. Centrosome and microtubule dynamics during meiotic progression in the mouse oocyte. Journal of Cell Science 1991; 100: 289-98.

Mintz B, Gearhart JD, Guymont AO. Phytohemagglutinin-mediated blastomere aggregation and development of allophenic mice. Developmental Biology 1973; 31: 195-9.

Misica-Turner PM, Oback FC, Eichenlaub M, Wells DN, Oback B. Aggregating embryonic but not somatic nuclear transfer embryos increases cloning efficiency in cattle. Biology of Reproduction 2007; 76: 268-78.

Montague TG, Cruz JM, Gagnon JA, Church GM, Valen E. CHOPCHOP: a CRISPR/Cas9 and TALEN web tool for genome editing. Nucleic acids research 2014: gku410.

Muir W. Comparison of genomic and traditional BLUP-estimated breeding value accuracy and selection response under alternative trait and genomic parameters. Journal of Animal Breeding and Genetics 2007; 124: 342-55.

Nagy A, Gocza E, Diaz EM, Prideaux V, Ivanyi E, Markkula M, Rossant J. Embryonic stem cells alone are able to support fetal development in the mouse. Development 1990; 110: 815-21.

Nagy A, Rossant J, Nagy R, Abramow-Newerly W, Roder JC. Derivation of completely cell culture-derived mice from early-passage embryonic stem cells. Proceedings of the National Academy of Sciences 1993; 90: 8424-8.

Nagy A, Gertsenstein M, Vintersten K, Behringer RR (2003) Manipulating the mouse embryo: a laboratory manual, 3 edn. Cold spring harbor laboratory press, Cold Spring Harbor, New York

Nganvongpanit K, Müller H, Rings F, Hoelker M, Jennen D, Tholen E, Havlicek V, Besenfelder U, Schellander K, Tesfaye D. Selective degradation of maternal and embryonic transcripts in in vitro produced bovine oocytes and embryos using sequence specific double-stranded RNA. Reproduction 2006; 131: 861-74.

Ni W, Qiao J, Hu S, Zhao X, Regouski M, Yang M, Polejaeva IA, Chen C. Efficient gene knockout in goats using CRISPR/Cas9 system. PloS one 2014; 9: e106718.

Nichols J, Zevnik B, Anastassiadis K, Niwa H, Klewe-Nebenius D, Chambers I, Schöler H, Smith A. Formation of pluripotent stem cells in the mammalian embryo depends on the POU transcription factor Oct4. Cell 1998; 95: 379-91.

Niwa H, Toyooka Y, Shimosato D, Strumpf D, Takahashi K, Yagi R, Rossant J. Interaction between Oct3/4 and Cdx2 determines trophectoderm differentiation. Cell 2005; 123: 917-29.

Nordhoff V, Hubner K, Bauer A, Orlova I, Malapetsa A, Scholer HR. Comparative analysis of human, bovine, and murine Oct-4 upstream promoter sequences. Mamm Genome 2001; 12: 309-17.

Oback B, Wiersema A, Gaynor P, Laible G, Tucker F, Oliver J, Miller A, Troskie H, Wilson K, Forsyth J. Cloned cattle derived from a novel zona-free embryo reconstruction system. Cloning & Stem Cells 2003; 5: 3-12.

Ohno S, Trujillo J, Stenius C, Christian L, Teplitz R. Possible germ cell chimeras among newborn dizygotic twin calves (Bos taurus). Cytogenetic and genome research 1962; 1: 258-65.

Palma G, Clement-Sengewald A, Berg U, Brem G. Role of the embryo number in the development of in-vitro produced bovine embryos. Theriogenology 1992; 37: 271.

Palmieri SL, Peter W, Hess H, Schöler HR. Oct-4 transcription factor is differentially expressed in the mouse embryo during establishment of the first two extraembryonic cell lineages involved in implantation. Developmental Biology 1994; 166: 259-67.

Pascoe WS, Kemler R, Wood SA. Genes and functions: trapping and targeting in embryonic stem cells. Biochimica et Biophysica Acta (BBA)-Reviews on Cancer 1992; 1114: 209-21.

Pfeffer PL. Lineage commitment in the mammalian preimplantation embryo. In: Reproduction in Domestic Ruminants VIII. Juengel JM, A; Price, C; Reynolds, LP; Smith, MF; Webb, R, ed.: Context 2014:

Picard L, Chartrain I, King WA, Betteridge KJ. Production of chimaeric bovine embryos and calves by aggregation of inner cell masses with morulae. Molecular reproduction and development 1990; 27: 295-304.

Ponsart C, Le Bourhis D, Knijn H, Fritz S, Guyader-Joly C, Otter T, Lacaze S, Charreaux F, Schibler L, Dupassieux D. Reproductive technologies and genomic selection in dairy cattle. Reproduction, Fertility and Development 2014; 26: 12-21.

Poueymirou WT, Auerbach W, Frendewey D, Hickey JF, Escaravage JM, Esau L, Doré AT, Stevens S, Adams NC, Dominguez MG. F0 generation mice fully derived from gene-targeted embryonic stem cells allowing immediate phenotypic analyses. Nature biotechnology 2007; 25: 91-9.

Ralston A, Rossant J. Cdx2 acts downstream of cell polarization to cell-autonomously promote trophectoderm fate in the early mouse embryo. Developmental Biology 2008; 313: 614-29.

Ralston A, Cox BJ, Nishioka N, Sasaki H, Chea E, Rugg-Gunn P, Guo G, Robson P, Draper JS, Rossant J. Gata3 regulates trophoblast development downstream of Tead4 and in parallel to Cdx2. Development 2010; 137: 395-403.

Reichenbach M, Lim T, Reichenbach H-D, Guengoer T, Habermann FA, Matthiesen M, Hofmann A, Weber F, Zerbe H, Grupp T. Germ-line transmission of lentiviral PGK-EGFP integrants in transgenic cattle: new perspectives for experimental embryology. Transgenic research 2010; 19: 549-56.

Repas-Humpe L, Humpe A, Lynen R, Glock B, Dauber E, Simson G, Mayr W, Köhler M, Eber S. A dispermic chimerism in a 2-year-old Caucasian boy. Annals of hematology 1999; 78: 431-4.

Rinkevich B. Human natural chimerism: an acquired character or a vestige of evolution? Human immunology 2001; 62: 651-7.

Roode M, Blair K, Snell P, Elder K, Marchant S, Smith A, Nichols J. Human hypoblast formation is not dependent on FGF signalling. Developmental Biology 2012; 361: 358-63.

Sakurai N, Takahashi K, Emura N, Fujii T, Hirayama H, Kageyama S, Hashizume T, Sawai K. The Necessity of OCT-4 and CDX2 for Early Development and Gene Expression Involved in Differentiation of Inner Cell Mass and Trophectoderm Lineages in Bovine Embryos. Cellular Reprogramming (Formerly" Cloning and Stem Cells") 2016;

Sander JD, Joung JK. CRISPR-Cas systems for editing, regulating and targeting genomes. Nature biotechnology 2014; 32: 347-55.

Sawai T, Yoshimoto M, Kinoshita EI, Baba T, Matsumoto T, Tsuji Y, Fukuda S, Harada N, Niikawa N. Case of 46, XX/47, XY,+ 21 chimerism in a newborn infant with ambiguous genitalia. American journal of medical genetics 1994; 49: 428-30.

Schaeffer L. Strategy for applying genome-wide selection in dairy cattle. Journal of Animal Breeding and Genetics 2006; 123: 218-23.

Schiffmacher AT, Keefer CL. CDX2 regulates multiple trophoblast genes in bovine trophectoderm CT-1 cells. Molecular reproduction and development 2013; 80: 826-39.

Schindelin J, Arganda-Carreras I, Frise E, Kaynig V, Longair M, Pietzsch T, Preibisch S, Rueden C, Saalfeld S, Schmid B. Fiji: an open-source platform for biological-image analysis. Nature methods 2012; 9: 676-82.

Schöler HR. Octamania: the POU factors in murine development. Trends in Genetics 1991; 7: 323-9.

Seidel G. Brief introduction to whole-genome selection in cattle using single nucleotide polymorphisms. Reproduction, Fertility and Development 2009; 22: 138-44.

Seruggia D, Montoliu L. The new CRISPR–Cas system: RNA-guided genome engineering to efficiently produce any desired genetic alteration in animals. Transgenic research 2014; 23: 707-16.

Simmet K, Reichenbach M, Reichenbach H-D, Wolf E. Phytohemagglutinin facilitates the aggregation of blastomere pairs from Day 5 donor embryos with Day 4 host embryos for chimeric bovine embryo multiplication. Theriogenology 2015a; 84: 1603-10.

Simmet K, Reichenbach M, Jung S, Fries R, Grupp T, Gschoederer C, Scherzer J, Reichenbach H, Wolf E (2015b) Phytohemagglutinin (PHA) influences blastocyst rate and contribution of donor cells to the inner cell mass of asynchronous bovine embryo aggregation chimeras. Reproduction in Domestic Animals. 16-

Simmet K, Reichenbach M, Jung S, Fries R, Grupp T, Gschöderer C, Scherzer J, Reichenbach H, Wolf E (2015c) 84 Pairs of blastomeres from bovine day 5 morulae are able to contribute to inner cell mass and trophectoderm in chimeric embryos generated by aggregation with two day 4 morulae. Reproduction, Fertility and Development. 135-

Simmet K, Klymiuk, N., Zakhartchenko, V., Güngör, T., Reichenbach, M., Reichenbach, H.D., & Wolf, E. (2016) OCT4 (POU5F1) has no influence on the ratio of inner cell mass to trophectodermal cells in cloned bovine day 7 blastocysts. In: 18th International Congress on Animal Reproduction, ICAR 2016, Tours, France

Song B-S, Kim J-S, Yoon S-B, Lee K-S, Koo D-B, Lee D-S, Choo Y-K, Huh J-W, Lee S-R, Kim S-U. Inactivated Sendai-virus-mediated fusion improves early development of cloned bovine embryos by avoiding endoplasmic-reticulum-stress-associated apoptosis. Reproduction, Fertility and Development 2011; 23: 826-36.

Sugimura S, Akai T, Hashiyada Y, Somfai T, Inaba Y, Hirayama M, Yamanouchi T, Matsuda H, Kobayashi S, Aikawa Y. Promising system for selecting healthy in vitro–fertilized embryos in cattle. PloS one 2012; 7: e36627.

Summers P, Shelton J, Bell K. Synthesis of primary Bos taurus-Bos indicus chimaeric calves. Animal Reproduction Science 1983; 6: 91-102.

Suwińska A, Czołowska R, Ożdżeński W, Tarkowski AK. Blastomeres of the mouse embryo lose totipotency after the fifth cleavage division: Expression of Cdx2 and Oct4 and developmental potential of inner and outer blastomeres of 16- and 32-cell embryos. Developmental Biology 2008; 322: 133-44.

Tagawa M, Matoba S, Narita M, Saito N, Nagai T, Imai K. Production of monozygotic twin calves using the blastomere separation technique and Well of the Well culture system. Theriogenology 2008; 69: 574-82.

Tarkowski AK. Mouse chimaeras developed from fused eggs. Nature 1961; 190: 857-60.

Tarkowski AK, Suwińska A, Czołowska R, Ożdżeński W. Individual blastomeres of 16-and 32-cell mouse embryos are able to develop into foetuses and mice. Developmental Biology 2010; 348: 190-8.

Tsunoda Y, Kato Y, Inui A (2006) Cloning in cattle. Taylor & Francis, London

Vajta G, Peura T, Holm P, Paldi A, Greve T, Trounson A, Callesen H. New method for culture of zona-included or zona-free embryos: The Well of the Well (WOW) system. Molecular reproduction and development 2000; 55: 256-64.

Vajta G, Lewis IM, Hyttel P, Thouas GA, Trounson AO. Somatic cell cloning without micromanipulators. Cloning 2001; 3: 89-95.

Van Eijk M, Van Rooijen M, Modina S, Scesi L, Folkers G, Van Tol H, Bevers M, Fisher S, Lewin H, Rakacolli D. Molecular cloning, genetic mapping, and developmental expression of bovine POU5F1. Biology of Reproduction 1999; 60: 1093-103.

Viuff D, Palsgaard A, Rickords L, Lawson LG, Greve T, Schmidt M, Avery B, Hyttel P, Thomsen PD. Bovine embryos contain a higher proportion of polyploid cells in the trophectoderm than in the embryonic disc. Molecular reproduction and development 2002; 62: 483-8.

Wang H, Yang H, Shivalila CS, Dawlaty MM, Cheng AW, Zhang F, Jaenisch R. One-step generation of mice carrying mutations in multiple genes by CRISPR/Cas-mediated genome engineering. Cell 2013; 153: 910-8.

Wang S, Panter K, Evans R, Bunch T. The effects of pokeweed mitogen (PWM) and phytohemagglutinin (PHA) on bovine oocyte maturation and embryo development in vitro. Animal Reproduction Science 2001; 67: 215-20.

Wang X, Dai J. Concise review: isoforms of OCT4 contribute to the confusing diversity in stem cell biology. Stem cells 2010; 28: 885-93.

Whitworth KM, Lee K, Benne JA, Beaton BP, Spate LD, Murphy SL, Samuel MS, Mao J, O'Gorman C, Walters EM. Use of the CRISPR/Cas9 system to produce genetically engineered pigs from in vitro-derived oocytes and embryos. Biology of Reproduction 2014; 91: 78.

Wu G, Han D, Gong Y, Sebastiano V, Gentile L, Singhal N, Adachi K, Fischedick G, Ortmeier C, Sinn M. Establishment of totipotency does not depend on Oct4A. Nature cell biology 2013; 15: 1089-97.

Wu G, Schöler HR. Role of Oct4 in the early embryo development. Cell Regeneration 2014; 3: 7.

Wu X, Song M, Yang X, Liu X, Liu K, Jiao C, Wang J, Bai C, Su G, Liu X, Li G. Establishment of bovine embryonic stem cells after knockdown of CDX2. Scientific reports 2016; 6: 28343.

Wuensch A, Habermann FA, Kurosaka S, Klose R, Zakhartchenko V, Reichenbach H-D, Sinowatz F, McLaughlin KJ, Wolf E. Quantitative monitoring of pluripotency gene activation after somatic cloning in cattle. Biology of Reproduction 2007; 76: 983-91.

Yamanaka Y, Lanner F, Rossant J. FGF signal-dependent segregation of primitive endoderm and epiblast in the mouse blastocyst. Development 2010; 137: 715-24.

Yen S-T, Zhang M, Deng JM, Usman SJ, Smith CN, Parker-Thornburg J, Swinton PG, Martin JF, Behringer RR. Somatic mosaicism and allele complexity induced by CRISPR/Cas9 RNA injections in mouse zygotes. Developmental Biology 2014; 393: 3-9.

Zakhartchenko V, Wolf E, Palma G, Brem G. Effect of donor embryo cell number and cell size on the efficiency of bovine embryo cloning. Molecular reproduction and development 1995; 42: 53-7.

Zhao X-y, Li W, Lv Z, Liu L, Tong M, Hai T, Hao J, Guo C-l, Ma Q-w, Wang L. iPS cells produce viable mice through tetraploid complementation. Nature 2009; 461: 86-90.

XI. Acknowledgements

I am very grateful to Prof. Dr. Eckhard Wolf for the opportunity to do my doctoral thesis at the Chair for Molecular Animal Breeding and Biotechnology (LMU-Munich) and for reviewing this manuscript. I would also like to thank Dr. Myriam Reichenbach, Dr. Horst-Dieter Reichenbach, PD Dr. Valeri Zakhartchenko and Dr. Nikolai Klymiuk very much for their endless support. Your great supervision and constant motivation enthused me throughout the whole time and made this work possible.

Thanks to all my colleagues at the Moorversuchsgut, especially the technical assistants (Ingrid, Eva, Tuna - thank you for your patience!) and my fellow graduate stundents (Michi, Sofia, Anna, Janet, Erica and Arne – thank you for a great time!).

I also want to thank Prof. Dr. Ulrike Gaul and Dr. Christophe Jung from the LMU Gene Center for introduction and access to confocal laser scanning microscopy.

Finally, I want to thank Franzi and my family and friends. Thank you for support, your interest and distraction!